

# Target motion analysis and track association with a network of proximity sensors

Régis Donati<sup>a</sup>, Jean-Pierre Le Cadre<sup>b,\*</sup>

<sup>a</sup> *Department of Undersea Warfare, DSA/SPN/STILSM, 8 bd Victor, 00303 Paris Armees, France*

<sup>b</sup> *IRISA/CNRS, Campus de Beaulieu, 35042 Rennes Cedex, France*

Received 23 August 2004; received in revised form 8 February 2005; accepted 8 February 2005

Available online 12 March 2005

## Abstract

Target motion analysis and track association are the aims of this paper. It is assumed that the target trajectory is only partially observable by using temporal processing of a single sensor. Thus, original algorithms have been developed for fusing local estimates. Though suboptimal, such algorithms are feasible and close to optimality. Their performances have been theoretically investigated.

Another problem is track-to-track association, the aim of which is to perform decision if the tracks estimated by two local sub-systems are related to a single target or not and for which an original approach has been developed. This study is illustrated by a specific case study: the detection of a moving target by stationary electric sensors.

© 2005 Elsevier B.V. All rights reserved.

**Keywords:** Target motion analysis; Detection; Network; Proximity sensors; Track fusion; Performance analysis

## 1. Introduction

Detection and target motion analysis are usually disconnected. It is generally assumed that detection has been achieved at a signal processing level, while target motion analysis is more relevant of information processing. Even if the aim of surveillance devices (e.g. sonar, radar systems) is to detect, track and classify a very large number of targets, the following problem has its own importance: *How to detect a (unique) target crossing a sensor network?*

Some remarks will enlighten the relevance of this problem. First, for many applications, the detection range of an elementary sensor is limited; thus a very reasonable assumption is that it can detect at most *one*

target, sufficiently close.<sup>1</sup> Second, due to this limited detection range, the interest of centralized processing may be seriously mitigated due to the fact that the signal-to-noise ratios are too much different and furthermore *unknown*. A practical consequence is that it is likely that a moving target can be perceived by *at most* one sensor of the network, at each time-period. Third, since spatial discrimination is not relevant in this context, the only way to detect at the sensor level is to use temporal processing so as to (partially) estimate the target motion. Detection at the network level will be achieved by gathering the *partial* target motion estimates for deciding if they have a common origin.

For the sake of simplicity, we shall mainly restrict to a rectilinear and uniform motion model. Of course, this is not restrictive but extensions are beyond this paper scope. The problem we consider is (relatively)

\* Corresponding author. Tel.: +33 2 99 84 72 24; fax: +33 2 99 84 71 71.

E-mail addresses: [regis.donati@dga.defense.gouv](mailto:regis.donati@dga.defense.gouv) (R. Donati), [lecadre@irisa.fr](mailto:lecadre@irisa.fr) (J.-P. Le Cadre).

<sup>1</sup> This point will be made more precise in Section 5 see the “cookie-cutter” sensor range.

independent of the sensor nature, which may be acoustic, magnetic, etc. The crucial point is that the elementary sensors are fixed and work in *passive* mode; thus, target motion model is only partially observed. This leads us to consider the following problem [3]: *how is it possible to fuse these partial estimates so as to jointly perform a complete estimation of the target trajectory and a track detection?*

This subject has been the object of fruitful research. Detection by a field of fixed sensors has been rather extensively considered in the search theory literature. We refer to the original work of Koopman [11] for a general and technical presentation. Additional insights can be found in [20,22]. Associating the partial estimates is another problem. Important contributions include the works of Mucci et al. and of La Scala and Farina [17]. The scopes of this paper and of the recent paper of Wettergren et al. [23] are rather similar. However, the information which is considered at the sensor level in [23] is *only* reduced to a CPA information. Authors then developed an original method for target tracking via geometric invariants.

For all these methods, performance analysis is an important concern. It has been investigated by La Scala and Farina [17,18], with interesting and insightful results. Here, our aim is to provide a general presentation of performance analysis of the fusion methods.

To illustrate these ideas, an original problem is presented. More specifically, we shall consider as an application the detection of an underwater moving target going through a network made of electric sensors. Actually, various phenomena such as galvanic corrosion between the hull and the propeller [1] will induce a static electric field known as the UEP (underwater electric potential) field [1]. In Section 2, the signal processing context is briefly presented. Of course, centralized processing is optimal from an idealized signal processing perspective. However, for reasons which have been presented above it is also irrelevant in this context. This is followed by a brief presentation of the calculation of the probability that the target be detected by at least one sensor of the array (Section 3).

Thus, fusion of partial target motion analysis (TMA) “*tracklets*” is considered in Section 4 in order to perform a complete estimation of the target trajectory from partial ones. Various fusion rules are examined. Under the assumption of correct association, their performances and advantages are analyzed and compared. However, a difficult problem remains: tracklet association and more specifically the validity of the unique track assumption. To that aim, an original tracklet distance is defined and its performance is analyzed. Then, testing for correct association is considered [5] in Section 5. Its aim is to test the association of partial tracks, estimated at the sensor level. Monte Carlo simulations show good agreement with theoretical prediction of performance.

*Principal notations:*

- FIM: the Fisher information matrix,
- $cpa$ : the closest distance from sensor to target,  $t_{cpa}$ : the time instant of CPA,  $d$  the intersensor distance,
- $\mathbf{X} = \{cpa, v, \theta, t_{cpa}\}$ : the complete target state vector,  $\mathbf{Y}(\mathbf{X}) = \{\alpha = \frac{cpa}{v}, \theta, t_{cpa}\}$  the partial target state vector,
- $A^T$ : the transpose of the  $A$  matrix,  $\mathcal{N}(\mathbf{X}, \Gamma)$  the normal distribution with mean  $\mathbf{X}$  and covariance matrix  $\Gamma$ ,
- $\langle \mathbf{X}, \mathbf{Y} \rangle$ : scalar product of the two vectors  $\mathbf{X}, \mathbf{Y}$ ,  $\|\mathbf{X}\|$ : norm of the  $\mathbf{X}$  vector,
- $\det(A)$  the determinant of a (square) matrix  $A$  (also denoted  $|A|$ ),
- $\hat{\mathbf{X}}_f$  corresponds to a fused estimator whatever the fusion method is,
- $P_D, P_{FA}, P_{FAS}$ : probability of detection, false alarm, false association.

## 2. Processing at the elementary receiver level

In this section, we shall briefly present a model for the (signal) processing at the elementary receiver level. Note that a model of the same type can be considered for acoustic sensors [2,16] and more generally passive proximity sensors. The presentation of this part is deliberately made short since its aim is only to provide a modelling of the low-level processing. More details about the expression of the analyzed signal (here electric field  $\mathbf{e}(t)$ ) can be found in [4], where it is also explained that  $\mathbf{e}(t)$  is a function of *three* parameters which are:

- the ratio  $\alpha \triangleq \frac{cpa}{v}$ ;  $cpa$  minimal target receiver distance,  $v$  target speed,
- the time of the closest distance target-receiver (CPA), denoted  $t_{cpa}$ ,
- the target heading  $\theta$ ,

so that the following spatio-temporal modelling of the sensor output is appropriate:

$$\mathbf{z}_t = \mathbf{e}(\mathbf{Y}, t) + \mathbf{n}_t, \quad \text{where } \mathbf{Y} = \left[ \alpha \triangleq \frac{cpa}{v}, t_{cpa}, \theta \right]^T. \quad (2.1)$$

A common feature of short-range sensors is that the received signal is modelled in terms of a specific target trajectory parameterization (denoted as CPA coordinates for the sequel), i.e.  $\{cpa, v, t_{cpa}, \theta\}$  (see Fig. 2). These coordinates which are well adapted to distributed networks are presented in Appendix A. Notice furthermore that the target trajectory is (generally) only partially observable, which means that the dimension of the observable space is three (i.e.  $\dim(\mathbf{Y})$ ).

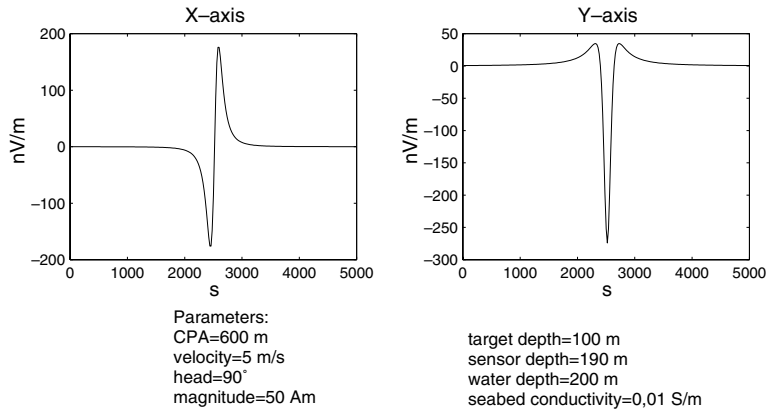


Fig. 1. Theoretical UEP signature of a moving source.

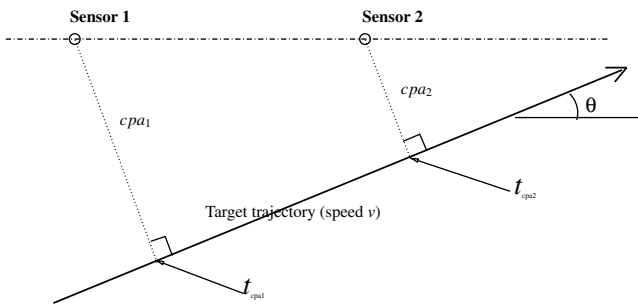


Fig. 2. Kinematic definitions and notations.

An example of the “theoretical” electric signature of a moving target is shown in Fig. 1. Notice the strong change which occurs at CPA. Defining the “signature”  $\mathbf{U}(\mathbf{Y})$  by normalization<sup>2</sup> of the UEP vector  $\mathcal{E}(\mathbf{Y})(\mathcal{E}(\mathbf{Y}) \triangleq K\mathbf{U}(\mathbf{Y}))$ , maximizing the likelihood reverts to finding

$$\hat{\mathbf{Y}} = \arg \max_{\mathbf{Y}} (\langle \mathbf{Z}, \mathbf{U}(\mathbf{Y}) \rangle)^2, \quad \hat{K} = \langle \mathbf{Z}, \mathbf{U}(\hat{\mathbf{Y}}) \rangle. \quad (2.2)$$

Thus, the parameter vector  $\hat{\mathbf{Y}}$  is estimated by selecting the normed signal  $\mathbf{U}(\mathbf{Y})$  which maximizes the energy of the projection of the observation vector  $\mathbf{Z}$  on the  $\{\mathbf{U}(\mathbf{Y})\}$  basis (matched filtering). Though stationarity hypothesis is clearly irrelevant for this type of problem,<sup>3</sup> it has been shown in [4] that the above estimates of the parameter vector  $\mathbf{Y} = (\alpha = \frac{cpa}{v}, \theta, t_{cpa})$  are asymptotically optimal. We refer to [15] for a presentation of the analysis of asymptotic performance in the non-stationary case. More precisely, denoting FIM the Fisher information matrix and  $\mathcal{N}$  the normal density, we have

$$[\hat{\mathbf{Y}} - \mathbf{Y}] \rightarrow \mathcal{N} \left( \begin{bmatrix} 0 \\ 0 \\ 0 \end{bmatrix}, [\text{FIM}_{\mathbf{Y}}]^{-1} \right), \quad (2.3)$$

<sup>2</sup> i.e.  $\mathbf{U}(\mathbf{Y}) = (1/\|\mathcal{E}(\mathbf{Y})\|)\mathcal{E}(\mathbf{Y})$ ,  $K$ : signal-to-noise ratio.

<sup>3</sup> Estimating the  $\mathbf{Y}$  vector is made possible only by the changes of observation means.

with

$$[\text{FIM}_{\mathbf{Y}}](i, j) = \left[ K^2 \left\langle \frac{\partial \mathbf{U}(\mathbf{Y})}{\partial Y_i}, \frac{\partial \mathbf{U}(\mathbf{Y})}{\partial Y_j} \right\rangle \right] \quad 1 \leq i, j \leq 3. \quad (2.4)$$

Actually, this type of modelling is quite general for proximity sensors. For instance, we know, it is shown (see Appendix A) that the effect of motion (Doppler effect) on an emitted signal (frequency  $f_0$ ) results in a frequency shift

$$f_i = f_0 \left( 1 - \frac{v \sin(\theta_i + \beta_i)}{c} \right), \quad (2.5)$$

( $c$ : wave velocity), where  $\beta_i$  is the target azimuth and  $\theta_i$  its heading, and where the temporal evolution of the bearing angle  $\beta_i$  is given by (see Appendix A)

$$\sin(\beta_i) = \frac{-\alpha \sin \theta + (t - t_{cpa}) \cos \theta}{\alpha \cos \theta + (t - t_{cpa}) \sin \theta}. \quad (2.6)$$

Then, it can be shown (see [19]) that the dimension of the observable space is three. Thus, this observable space can be parameterized by the *partial* CPA coordinates  $\{\frac{cpa}{v}, \theta, t_{cpa}\}$ . Let us stress that there is a 1:1 correspondence between Cartesian coordinates and CPA ones (see Appendix A). The principal motivation for introducing CPA coordinates is that it is the *natural* parameterization of the *observable* space for a proximity sensor (see Appendix A).

Let us go now to the general setting of the problem. The basic scenario we shall consider is made of two sensors observing the same moving target, as depicted in Fig. 2. Throughout this paper, it is assumed that the target motion is rectilinear and uniform.

The first way to process the observations collected by the two sensors is to consider them as a whole and to apply matched filtering to this concatenated observation  $\mathbf{Z}$  ( $\mathbf{Z} = (\mathbf{Z}_1^T, \mathbf{Z}_2^T)^T$ ). This is the *centralized processing*. The observation is then modelled as

$$\mathbf{Z} = \mathcal{E}(\mathbf{X}) + \mathbf{N} = \begin{pmatrix} \mathcal{E}(\mathbf{Y}_1(\mathbf{X})) \\ \mathcal{E}(\mathbf{Y}_2(\mathbf{X})) \end{pmatrix} + \begin{pmatrix} \mathbf{N}_1 \\ \mathbf{N}_2 \end{pmatrix},$$

where

$$\begin{aligned} \mathbf{X} &= (cpa_1, v, \theta, t_{cpa_1})^T, \\ \mathbf{Y}_1(\mathbf{X}) &= (\alpha_1 \triangleq cpa_1/v, \theta, t_{cpa_1})^T, \\ \mathbf{Y}_2(\mathbf{X}) &= (\alpha_2 \triangleq cpa_2/v, \theta, t_{cpa_2})^T, \\ \alpha_2 &= \alpha_1 - (d/v) \sin \theta, t_{cpa_2} = t_{cpa_1} + (d/v) \cos \theta. \end{aligned} \quad (2.7)$$

Unfortunately, the centralized processing suffers from serious drawbacks. Among them are computation and, overall, communication requirements. More fundamentally is the fact that for short range sensors, the decrease of the signal-to-noise ratio as a range function makes that if a sensor “sees” the target, it is undetected by most of the other ones (see Section 3). Practically, this means that the useful information, i.e. a target is in the range detection of a proximity sensor is “diluted” in noise only observations. Furthermore, it is not realistic that reliable modelling of the signal-to-noise ratios are available at each time-period and for each sensor. This is a very fundamental difference with “classical” array processing and the basic motivation of this paper.

Nevertheless, it will play the role of the idealized reference. Rather surprisingly, we will show that suboptimal (distributed) processing is very close to optimality, while having definite advantages.

Thus, our general aim will be the association of the outputs of the elementary receivers so as to have an estimation of the complete trajectory vector  $\mathbf{X}$  ( $\mathbf{X} = (cpa, v, \theta, t_{cpa})^T$ ) from the partial estimates obtained on each sensor. Using elementary calculations.<sup>4</sup> The following deterministic formulas are then straightforwardly deduced from Eqs. (A.1) and (A.2):

$$\frac{cpa_2}{v} = \alpha_2 = \alpha_1 - \frac{d}{v} \sin(\theta), \quad (2.8)$$

$$t_{cpa_2} = t_{cpa_1} + \frac{d}{v} \cos(\theta),$$

as well as the statistical distribution of the partial target trajectory estimates

$$\begin{aligned} \begin{pmatrix} \hat{\alpha}_1 \\ \hat{\theta}_1 \\ \hat{t}_{cpa_1} \end{pmatrix} &\rightarrow \mathcal{N} \left[ \begin{pmatrix} \alpha_1 \\ \theta \\ t_{cpa_1} \end{pmatrix}; \Gamma_1 \right], \\ \begin{pmatrix} \hat{\alpha}_2 \\ \hat{\theta}_2 \\ \hat{t}_{cpa_2} \end{pmatrix} &\rightarrow \mathcal{N} \left[ \begin{pmatrix} \alpha_2 \\ \theta \\ t_{cpa_2} \end{pmatrix}; \Gamma_2 \right]. \end{aligned} \quad (2.9)$$

From now on, we shall consider that the vectors of partial estimates  $\hat{\mathbf{Y}}_1 \triangleq (\hat{\alpha}_1, \hat{\theta}_1, \hat{t}_{cpa_1})^T$  and  $\hat{\mathbf{Y}}_2 \triangleq (\hat{\alpha}_2, \hat{\theta}_2, \hat{t}_{cpa_2})^T$

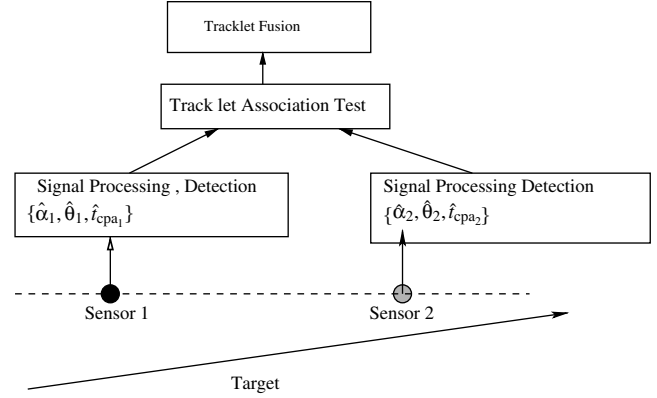


Fig. 3. The multilevel distributed processing.

as the *observations*. As it is a reasonable assumption to consider them as uncorrelated, they will be called “*tracklets*”. If the observation vectors  $\hat{\mathbf{Y}}_1$  and  $\hat{\mathbf{Y}}_2$  corresponds to the observation of the *same* target, then the following relations hold true:

$$\begin{aligned} \hat{\mathbf{Y}}_1 &= \mathbf{Y}_1(\mathbf{X}) + \mathbf{N}_1, \quad \hat{\mathbf{Y}}_2 = \mathbf{Y}_2(\mathbf{X}) + \mathbf{N}_2, \\ \mathbf{Y}_2(\mathbf{X}) &= \mathbf{Y}_1(\mathbf{X}) + \begin{pmatrix} -\frac{d}{v} \sin(\theta) \\ 0 \\ \frac{d}{v} \cos(\theta) \end{pmatrix}, \end{aligned} \quad (2.10)$$

where  $\mathbf{X}$  is the *complete* target trajectory parameterization. Thus, the problem we have to solve is twofold. In a first step it is necessary to estimate the  $\mathbf{X}$  vector from  $\hat{\mathbf{Y}}_1$  and  $\hat{\mathbf{Y}}_2$ . Under the perfect association hypothesis, this is achieved by fusing either partially (the  $\{\hat{\alpha}_{1,2}\}$ , or the  $\{\hat{t}_{cpa_{1,2}}\}$ ), or both (the track association fusion rule) or optimally (i.e. the whole set of parameters). The second step is to test the validity of associating the vectors  $\hat{\mathbf{Y}}_1$  and  $\hat{\mathbf{Y}}_2$ , which means: does they correspond to a unique target? It is worth noting that these two steps cannot be separated. An overview of the elementary case study is provided in Fig. 3. A preliminary step is to consider the detection of a moving target as a function of the sensor array characteristics. This is the object of the (short) next section.

### 3. Detection with an array of sensors

The aim of this section is to determine the detection performance of a network made of identical sensors, each one using the GLRT<sup>5</sup> test (see Eq. (2.2) and [4]) with the same threshold. Since this preliminary state is a fundamental prerequisite before associating and testing, it deserves some interest, exemplified by recent publications on this subject [14,23]. First, let us precise the objective we have in mind.

<sup>4</sup> Change from Cartesian to CPA coordinates is detailed in Appendix A.

<sup>5</sup> GLRT: Generalized Likelihood Test.

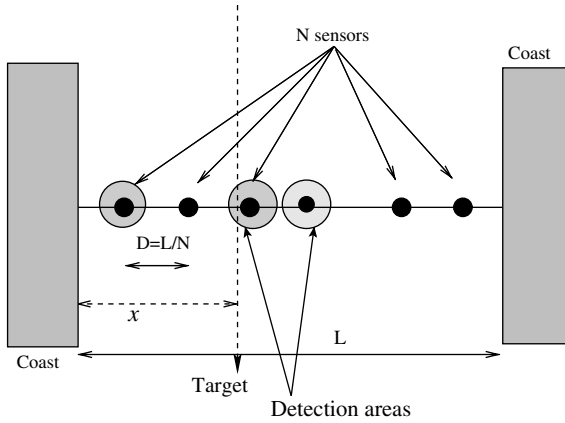


Fig. 4. The linear network and the lateral range disks.

**Definition 1.** A (moving) target is said detected by the sensor network if it has been detected by at least one sensor.

Of course, other definitions are possible; e.g. a majority rule, etc. But, the framework would be identical though more complicated. The network we will study is depicted in Fig. 4. So, it is simply a linear array (strait interdiction) made of  $N$  equispaced sensors.

Thus, in this way, sensor “cooperation” is made as elementary as possible. Our objective is to fix the  $P_{FA}$  of the whole sensor network at a given level ( $P_{FA,array} = \eta$ ). Assuming independent noises on the various sensors, we have

$$P_{FA,array} = 1 - \text{Prob.}[\text{no sensor generates a false alarm}] = 1 - (1 - P_{FA,sensor})^N. \tag{3.1}$$

So, in order that  $P_{FA,array}$  be at the fixed level, it is necessary to impose

$$P_{FA,sensor} = 1 - (1 - \eta)^{\frac{1}{N}} \approx \frac{\eta}{N}. \tag{3.2}$$

From this relation, it is then possible to infer the detection threshold we must apply on each sensor. To investigate the detection capabilities of the sensor network, we shall define now the typical target characteristics. A reasonable assumption is that it is going right on the network, with a heading close to  $90^\circ$ . Moreover, its speed is approximately known (mechanical and discretion constraints) as well as its electric momentum (the value of the SNR  $K$ ).

The target trajectory is thus parameterized by the abscissa (denoted  $x$ ) of its intersection with the array line. In the absence of specific information,  $X$  (which is the random variable associated with  $x$ ) can be supposed uniformly distributed in the interval  $[0, L]$ . Recalling the expression of the elementary probability of detection for a unique sensor (see Section 3), we deduce that the probability of detection for a sensor located at the abscissa  $id$  ( $d$ : elementary intersensor distance) is

$$P_{D,sensor_i}(x) = \int_{\eta}^{\infty} \chi_4^2(K^2(x - id), u) du, \tag{3.3}$$

$K$  given by Eq. (2.2).

This expression can be used to plot the so-called lateral range curve [20]. This curve gives, for a typical target, the probability of detecting a moving target as a function of the  $cpa$  parameter sensor (for a given probability of false alarm), for a *unique* sensor. For example, such a curve is plotted on Fig. 5(left) for a target defined by

- electric momentum: 50 A m, noise variances:  $200n \text{ V}^2/\text{m}^2$ ;
- speed: 5 m/s, heading:  $90^\circ$ ;

when the false alarm rate is 0.01.

Using the independence assumption for the noises incoming the various sensors, we obtain the detection

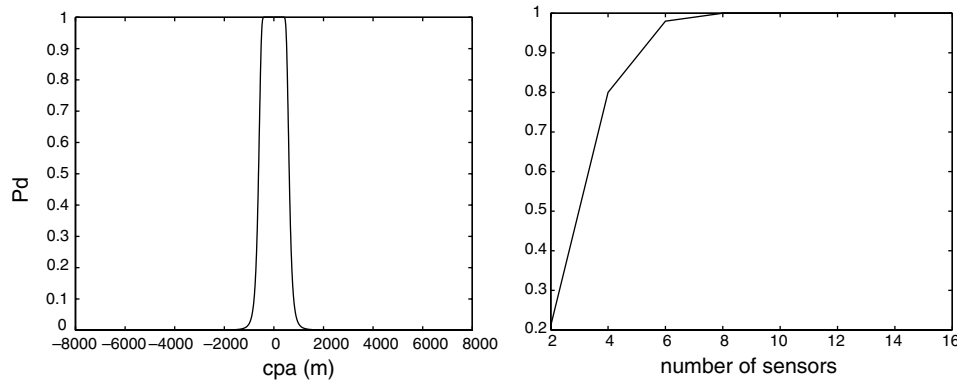


Fig. 5. (left) Lateral range curve: probability of detection ( $y$ -axis) versus range ( $x$ -axis) fixed  $P_{FA}$ , SNR and (right)  $P_{D,array}$  as a function of the sensor number (see Fig. 4).

probability of the whole array for a target crossing it at  $X = x$ :

$$P_{D,\text{array}}(x) = 1 - \text{Prob}[\text{no sensor detect.}], \quad (3.4)$$

$$1 - \prod_{i=1}^N \left[ 1 - \int_{\eta}^{\infty} \chi_4^2(K^2(x - id), u) du \right]. \quad (3.5)$$

Then, as  $X$  is uniformly distributed along  $[0, L]$ , the detection probability of the whole array for a typical target supposed to cross it anywhere stands as follows:

$$P_{D,\text{array}} = 1 - \frac{1}{L} \int_0^L \prod_{i=1}^N \left[ 1 - \int_{\eta}^{\infty} \chi_4^2(K^2(x - id), u) du \right] dx. \quad (3.6)$$

We note that the global probability of detection depends on the desired global false alarm probability and of the number of sensors. So, it is possible to determine the sensor number we need for protecting an area of length  $L$  against a typical target, with a given probability of detection and a fixed global false alarm probability. The detection probability of the array is represented on Fig. 5(right) as a function of the number of sensors. Parameters are those of Fig. 5(left), with  $L = 8000$  m and a global  $P_{FA}$  of  $10^{-1}$ .

This type of curve can be used in order to predict the performance of a given network relatively to a typical target or to determine the required number of sensors in order to achieve a given level of performance (for a given area and for a typical target). In fact, a rough “explanation” of Fig. 5(right) is provided by Figs. 4 and 5(left). The receiver detects in a “cookie-cutter” fashion [11,20]. So, the global probability of the array is rapidly increasing when the elementary detection disks become closer.

Actually, the detection process has been very roughly modelled in this section. Practically, sensors are able to provide much more than a “simple” detection (i.e. a binary information). They can provide partial estimates of the target trajectories as well as an estimation of their accuracies. The problem is now to fuse these (partial) estimates so as to consider jointly target detection and motion analysis at the network level. This will be the object of the incoming sections.

#### 4. Fusing local estimates (tracklets)

The problem we have to deal now is to fuse the local estimates (tracklets) for inferring an estimation of the complete target state. Thus, various approaches are considered, with various advantages and disadvantages. Such comparison relies essentially on performance analysis which constitutes an important contribution of this section. Section is organized as follows:

- Fusion of local estimates of the  $\alpha = cpa/v$  ratios.
- Fusion of local estimates of  $t_{cpa}$ .
- The (symmetric) track association fusion.
- The optimal fusion.

##### 4.1. Fusion of local estimates of the $\alpha = cpa/v$ ratios

Our aim is to obtain an *explicit* estimate (say  $\hat{\mathbf{X}}$ ) of the complete state vector from the partial ones, estimated at the sensor level. Let us detail now the various steps of this approach. From the local estimates of the target heading on sensor 1 and 2 (say  $\hat{\theta}_1$  and  $\hat{\theta}_2$ ), we deduce the following (fused) estimate (say  $\hat{\theta}_f$ ):

$$\hat{\theta}_f = \frac{1}{\sigma_{\theta_1}^2 + \sigma_{\theta_2}^2} (\sigma_{\theta_2}^2 \hat{\theta}_1 + \sigma_{\theta_1}^2 \hat{\theta}_2). \quad (4.1)$$

From the deterministic relation  $v = \frac{d \sin(\theta)}{\alpha_1 - \alpha_2}$  (see Eq. (2.8)), the following speed estimator  $\hat{v}$  is considered:

$$\hat{v}_f = \frac{d \sin(\hat{\theta}_f)}{\hat{\alpha}_1 - \hat{\alpha}_2}, \quad (4.2)$$

$\hat{\theta}_f$  being given by (4.1). The parameter  $v$  being estimated,  $cpa_1$  is trivially (though suboptimally) estimated from

$$\widehat{cpa}_1 = \hat{v}_f \hat{\alpha}_1 = \hat{\alpha}_1 \frac{d \sin(\hat{\theta}_f)}{\hat{\alpha}_1 - \hat{\alpha}_2}. \quad (4.3)$$

So that, finally, this fusion rule takes the following form ( $d$ : intersensor distance):

$$\hat{\theta}_f = \frac{1}{\sigma_{\theta_1}^2 + \sigma_{\theta_2}^2} (\sigma_{\theta_2}^2 \hat{\theta}_1 + \sigma_{\theta_1}^2 \hat{\theta}_2) \rightarrow \hat{v}_f = \frac{d \sin(\hat{\theta}_f)}{\hat{\alpha}_1 - \hat{\alpha}_2}, \quad (\widehat{cpa}_1)_f, \quad (\hat{t}_{cpa_1}). \quad (4.4)$$

We have just obtained a simple estimator of the complete target state vector  $\mathbf{X}$ . Even if this estimator cannot pretend to optimality, it has the advantage to be explicit and its performance can be calculated by means of elementary calculations. For that aim, we consider the following first-order expansions<sup>6</sup>:

$$\begin{aligned} \hat{\theta}_f &\stackrel{1}{=} \theta + \varepsilon_{\theta}, \\ \hat{v}_f &= \frac{d \sin(\hat{\theta}_f)}{(\hat{\alpha}_1 - \hat{\alpha}_2)} = \frac{d \sin(\hat{\theta}_f)}{(\alpha_1 + \varepsilon_{\alpha_1} - \alpha_2 - \varepsilon_{\alpha_2})} \\ &\stackrel{1}{=} v + \frac{d \cos(\theta)}{(\alpha_1 - \alpha_2)} \varepsilon_{\theta} - v \left( \frac{\varepsilon_{\alpha_1} - \varepsilon_{\alpha_2}}{\alpha_1 - \alpha_2} \right). \end{aligned} \quad (4.5)$$

This last approximation is not valid if the target trajectory is parallel to the array. Indeed, in this case, the ratios  $\alpha = (cpa/v)$  are identical with a zero difference. So, this fusion rule is of no interest when the target heading

<sup>6</sup> The symbol  $\stackrel{1}{=}$  means *first-order expansion*. Note that first-order expansion is generally sufficient for approximating the variance of an estimator; while a second-order expansion is a prerequisite for estimating the bias.

is close to 0 degree. If the target heading is reasonably far from 0 degree, we can derive from Eq. (4.3) the following equalities:

$$\begin{aligned} \widehat{cpa}_{1f} &= \hat{\alpha}_1 \frac{d \sin(\hat{\theta}_f)}{(\hat{\alpha}_1 - \hat{\alpha}_2)}, \\ &\stackrel{1}{=} cpa_1 + v\varepsilon_{\alpha_1} + \alpha_1 \left[ \frac{d \cos(\theta)}{\alpha_1 - \alpha_2} \varepsilon_\theta - v \frac{\varepsilon_{\alpha_1} - \varepsilon_{\alpha_2}}{\alpha_1 - \alpha_2} \right]. \end{aligned} \quad (4.6)$$

Collecting and rewriting the preceding expansions in a matrix form, the asymptotic performance of this  $\mathbf{X}$  estimate is

$$\begin{pmatrix} \widehat{cpa}_{1f} \\ \hat{v}_f \\ \hat{\theta}_f \\ \hat{t}_{cpa_1} \end{pmatrix} \rightarrow \mathcal{N} \left[ \begin{pmatrix} cpa_1 \\ v \\ \theta \\ t_{cpa_1} \end{pmatrix}; M_1 \Gamma_1 M_1^T + M_2 \Gamma_2 M_2^T \right], \quad (4.7)$$

where

$$M_1 = \begin{pmatrix} -v \left( \frac{\alpha_2}{\alpha_1 - \alpha_2} \right) & \frac{\alpha_1 d \cos(\theta)}{\alpha_1 - \alpha_2} \frac{\sigma_{\theta_2}^2}{\sigma_{\theta_1}^2 + \sigma_{\theta_2}^2} & 0 \\ -\frac{v}{\alpha_1 - \alpha_2} & \frac{d \cos(\theta)}{\alpha_1 - \alpha_2} \frac{\sigma_{\theta_2}^2}{\sigma_{\theta_1}^2 + \sigma_{\theta_2}^2} & 0 \\ 0 & \frac{\sigma_{\theta_2}^2}{\sigma_{\theta_1}^2 + \sigma_{\theta_2}^2} & 0 \\ 0 & 0 & 1 \end{pmatrix}$$

and

$$M_2 = \begin{pmatrix} v \left( \frac{\alpha_1}{\alpha_1 - \alpha_2} \right) & \frac{\alpha_1 d \cos(\theta)}{\alpha_1 - \alpha_2} \frac{\sigma_{\theta_1}^2}{\sigma_{\theta_1}^2 + \sigma_{\theta_2}^2} & 0 \\ \frac{v}{\alpha_1 - \alpha_2} & \frac{d \cos(\theta)}{\alpha_1 - \alpha_2} \frac{\sigma_{\theta_1}^2}{\sigma_{\theta_1}^2 + \sigma_{\theta_2}^2} & 0 \\ 0 & \frac{\sigma_{\theta_1}^2}{\sigma_{\theta_1}^2 + \sigma_{\theta_2}^2} & 0 \\ 0 & 0 & 0 \end{pmatrix}. \quad (4.8)$$

In the above equation, the  $\Gamma_i$  ( $i = 1, 2$ ) matrices are unknown. However, a reasonable assumption is that they can be tightly approximated by the Fisher Information matrices  $FIM_{\hat{\mathbf{Y}}_i}$ , where  $\hat{\mathbf{Y}}_i$  is itself given as a solution of the maximization problem (2.2). Note that these matrices are considered at the signal processing level (see Fig. 3). Estimating the FIM requires to estimate the SNR factor  $K^2$  ((2.4) and see [4]), which may be achieved by means of a standard time series method (regression) once  $\hat{\mathbf{X}}$  has been obtained.

Now, to investigate the performance of the fusion rule the volume of the covariance matrix of  $\hat{\mathbf{X}}$  is insightful and the following result is particularly appealing.

**Proposition 1.** Consider the uncertainty volume related to the (cpa/v) fusion rule, then the following results hold: The covariance matrix of  $\hat{\mathbf{X}}_f$  is approximated by the matrix  $M_1 \Gamma_1 M_1^T + M_2 \Gamma_2 M_2^T$  (see Eq. (4.8)) whose determinant can be factored as:

$$\begin{aligned} \text{If } \Gamma_1 = \Gamma_2 = \Gamma, \\ \text{then } \det(M_1 \Gamma M_1^T + M_2 \Gamma M_2^T) \\ = \varphi(\Gamma) \det(M_1 M_1^T + M_2 M_2^T), \end{aligned}$$

so that

$$\det(M_1 \Gamma M_1^T + M_2 \Gamma M_2^T) = \varphi(\Gamma) \left[ \frac{v^4}{(\alpha_1 - \alpha_2)^2} \right], \quad (4.9)$$

and, more generally,

$$\begin{aligned} \det(M_1 \Gamma_1 M_1^T + M_2 \Gamma_2 M_2^T) \\ = \varphi(\Gamma_1, \Gamma_2) \left[ \frac{(\sigma_{\theta_1}^4 + \sigma_{\theta_2}^4) v^4}{(\alpha_1 - \alpha_2)^2 (\sigma_{\theta_1}^2 + \sigma_{\theta_2}^2)^2} \right]. \end{aligned}$$

The functionals  $\varphi(\Gamma)$  and  $\varphi(\Gamma_1, \Gamma_2)$  are only related to the signal processing performance.

For a proof, we refer to Appendix B. The importance of the above result is that the effects of the signal processing performance (the  $\Gamma$  matrix) on the one hand, and of the fusion step on the other, appear clearly separated. This result is not fortuitous and is tightly related to basic results of multilinear algebra (see Appendix B). Another important consequence is the expression of the scalar functional  $\varphi(\Gamma)$ . For instance, elementary calculations yield the following results:

if  $\Gamma = \text{diag}(a, b, c)$ ,

$$\text{then } \varphi(\Gamma) = \frac{1}{4} a^2 b c (a = \sigma_\alpha^2, b = \sigma_\theta^2, c = \sigma_{t_{cpa}}^2),$$

if  $\Gamma = \text{Toeplitz}(a, b, c)$ ,

$$\begin{aligned} \text{then } \varphi(\Gamma) &= \frac{1}{4} ((a - c)(2a^3 - 3ab^2 + 2a^2c - b^2c)) \\ &\times (\sigma_{\theta_1} = \sigma_{\theta_2}), \end{aligned}$$

if  $\Gamma_1 = \text{diag}(a, b, c)$  and  $\Gamma_2 = \text{diag}(a', b', c)$ ,

$$\text{then } \varphi(\Gamma_1, \Gamma_2) = \frac{1}{4} a a' \left( \frac{b + b'}{2} \right) c. \quad (4.10)$$

Even if the effect of the target-receiver basis is clearly stated in Proposition 1 (the  $v^4/(\alpha_1 - \alpha_2)^2$  term), the function  $\varphi(\Gamma)$  emphasizes the influence of the quality of estimation of the  $\mathbf{Y}_i$  components. An interesting consequence is that the fusion rule can be chosen so as to minimize  $\varphi(\Gamma)$ . Finally, under the assumption  $\Gamma = \text{diag}(a, b, c)$  the asymptotic variance of the  $\hat{\mathbf{X}}$  components are given by ( $\sigma_{\theta_1} = \sigma_{\theta_2}$ )

$$\begin{aligned}\text{var}(\widehat{cpa}_1) &= \frac{2a(cpa_1^2 + cpa_2^2)v^2 + cpa_1^2bd^2(\cos(\theta))^2}{2(cpa_1 - cpa_2)^2}, \\ \text{var}(\hat{v}) &= \frac{4av^4 + bd^2v^2(\cos(\theta))^2}{2(cpa_1 - cpa_2)^2}, \\ \text{var}(\hat{\theta}) &= \frac{b}{2}, \quad \text{var}(\hat{t}_{cpa_1}) = c.\end{aligned}\quad (4.11)$$

Though effect of the CPA fusion on  $\text{var}(\hat{\theta})$  and  $\text{var}(\hat{t}_{cpa_1})$  is not surprising, effects on unobserved parameters (i.e.  $\text{var}(\widehat{cpa}_1)$  and  $\text{var}(\hat{v})$ ) are much more informative. In particular, importance of the  $(cpa_1 - cpa_2)$  term is put in evidence. To end this section, it remains to approximate the bias of this fusion rule. A second-order expansion of  $\hat{v}$  and  $\widehat{cpa}_1$  yields

$$\text{Bias}(\hat{\mathbf{X}}_{(cpa/v)}) = \left(2\frac{v^2}{d^2\sin^2(\theta)}\sigma_x^2 - \frac{1}{2}\sigma_\theta^2\right) \begin{pmatrix} 0 \\ v \\ cpa_1 \\ 0 \end{pmatrix}.\quad (4.12)$$

A similar expression holds for the  $t_{cpa}$  fusion rule. Considering Eqs. (4.12) and (4.11), we note that the effect of the bias may be not negligible versus variance ones.

#### 4.2. Fusion of local estimates of $t_{cpa}$

The other approach is valid when the target trajectory is approximately parallel to the array line and is based upon the fusion of the two estimates  $\hat{t}_{cpa_1}$  and  $\hat{t}_{cpa_2}$ . To be more precise, from the deterministic relation (see Eq. (2.8))  $t_{cpa_2} = t_{cpa_1} + \frac{d}{v}\cos(\theta)$ , we deduce

$$v = \frac{d\cos(\theta)}{t_{cpa_2} - t_{cpa_1}},$$

and the following estimators of the target velocity and  $cpa$ :

$$\begin{aligned}\hat{v}_f &= \frac{d\cos(\hat{\theta}_f)}{\hat{t}_{cpa_2} - \hat{t}_{cpa_1}}, \\ \widehat{cpa}_{1f} &= \hat{\alpha}_1 \frac{d\cos(\hat{\theta}_f)}{\hat{t}_{cpa_2} - \hat{t}_{cpa_1}}.\end{aligned}$$

So, that the whole algorithm takes the following form:

$$\begin{aligned}\hat{\theta}_f &= \frac{1}{\sigma_{\hat{\theta}_1}^2 + \sigma_{\hat{\theta}_2}^2}(\sigma_{\hat{\theta}_2}^2\hat{\theta}_1 + \sigma_{\hat{\theta}_1}^2\hat{\theta}_2) \rightarrow \hat{v}_f = \frac{d\cos(\hat{\theta}_f)}{\hat{t}_{cpa_2} - \hat{t}_{cpa_1}}, \\ \widehat{cpa}_{1f} &(\hat{t}_{cpa_1}).\end{aligned}\quad (4.13)$$

In order to calculate the performance of this estimator we consider again expansions relatively to the elementary errors, yielding

$$\begin{aligned}\hat{v} &= \frac{d\cos(\theta + \varepsilon_\theta)}{(t_{cpa_2} + \varepsilon_{t_{cpa_2}} - t_{cpa_1} + \varepsilon_{t_{cpa_1}})} \\ &\stackrel{1}{=} v - \frac{d\sin\theta}{t_{cpa_2} - t_{cpa_1}}\varepsilon_\theta - v\left(\frac{\varepsilon_{t_{cpa_2}} - \varepsilon_{t_{cpa_1}}}{t_{cpa_2} - t_{cpa_1}}\right).\end{aligned}\quad (4.14)$$

Assuming that the source heading is not close to  $90^\circ$ , the following approximation also holds:

$$\begin{aligned}\widehat{cpa}_1 &= \hat{\alpha}_1 \frac{d\cos\hat{\theta}}{(\hat{t}_{cpa_2} - \hat{t}_{cpa_1})} \\ &\stackrel{1}{=} cpa_1 + v\varepsilon_{\alpha_1} + \alpha_1\left(-\frac{d\sin\theta}{(t_{cpa_2} - t_{cpa_1})}\varepsilon_\theta - v\frac{\varepsilon_{t_{cpa_2}} - \varepsilon_{t_{cpa_1}}}{t_{cpa_2} - t_{cpa_1}}\right).\end{aligned}\quad (4.15)$$

Again, assuming normality of  $\hat{\mathbf{X}}$ , we have

$$\begin{pmatrix} \widehat{cpa}_1 \\ \hat{v} \\ \hat{\theta} \\ \hat{t}_{cpa_1} \end{pmatrix} \rightarrow \mathcal{N}\left[\begin{pmatrix} cpa_1 \\ v \\ \theta \\ t_{cpa_1} \end{pmatrix}; M'_1\Gamma_1M'^1_T + M'_2\Gamma_2M'^2_T\right],\quad (4.16)$$

where (under the assumption  $\sigma_{\theta_1} = \sigma_{\theta_2}$ )

$$M'_1 = \begin{pmatrix} v & -\frac{1}{2}\left(\frac{\alpha_1 d\sin\theta}{t_{cpa_2} - t_{cpa_1}}\right) & \frac{\alpha_1 v}{t_{cpa_2} - t_{cpa_1}} \\ 0 & -\frac{1}{2}\left(\frac{d\sin\theta}{t_{cpa_2} - t_{cpa_1}}\right) & \frac{v}{t_{cpa_2} - t_{cpa_1}} \\ 0 & \frac{1}{2} & 0 \\ 0 & 0 & 1 \end{pmatrix}\quad (4.17)$$

and

$$M'_2 = \begin{pmatrix} v & -\frac{1}{2}\left(\frac{\alpha_1 d\sin\theta}{t_{cpa_2} - t_{cpa_1}}\right) & -\frac{\alpha_1 v}{t_{cpa_2} - t_{cpa_1}} \\ 0 & -\frac{1}{2}\left(\frac{d\sin\theta}{t_{cpa_2} - t_{cpa_1}}\right) & \frac{-v}{t_{cpa_2} - t_{cpa_1}} \\ 0 & \frac{1}{2} & 0 \\ 0 & 0 & 0 \end{pmatrix}.\quad (4.18)$$

Quite analogously to (1), the following property holds for the  $t_{cpa}$ -based fusion rule.

**Proposition 2.** Assume that the covariance matrices  $\Gamma_1$  and  $\Gamma_2$  are equal ( $\Gamma_1 = \Gamma_2 = \Gamma$ ), then we have

$$\begin{aligned}\det(M'_1\Gamma M'^1_T + M'_2\Gamma M'^2_T) \\ = \varphi(\Gamma)\det(M'_1M'^1_T + M'_2M'^2_T),\end{aligned}$$

so that

$$\det(M'_1\Gamma M'^1_T + M'_2\Gamma M'^2_T) = \varphi(\Gamma)\left[\frac{v^4}{(t_{cpa_1} - t_{cpa_2})^2}\right].\quad (4.19)$$

Proof is omitted since identical to that of Proposition 1. This time, it is the difference  $(t_{cpa_1} - t_{cpa_2})$  term which is predominant.



### 4.3. The track association fusion rule

Up to now, we have considered the  $cpa$  as well as the  $t_{cpa}$  fusion rules. So, it seems quite desirable to use them jointly and in a symmetric way. Moreover, this fusion rule is especially relevant for testing the validity of the unique track assumption. So, let us consider the following  $F(v, \theta)$  functional:

$$F(v, \theta) \triangleq \left( \hat{\alpha}_2 - \hat{\alpha}_1 + \frac{d}{v} \sin(\theta) \right)^2 + \left( \hat{t}_{cpa_2} - \hat{t}_{cpa_1} - \frac{d}{v} \cos(\theta) \right)^2$$

and define  $\{\hat{\theta}_f, \hat{v}_f\} \in \arg \min_{\theta, v} F(v, \theta)$ . (4.20)

Minimizing  $F(v, \theta)$  with respect to  $v$  alone, a straightforward calculation yields

$$\hat{v}_f = \frac{d}{(\hat{t}_{cpa_2} - \hat{t}_{cpa_1}) \cos(\theta) - (\hat{\alpha}_2 - \hat{\alpha}_1) \sin(\theta)},$$

so that, after immediate simplifications, we obtain

$$F(\hat{v}_f, \theta) = [(\hat{\alpha}_2 - \hat{\alpha}_1) \cos(\theta) + (\hat{t}_{cpa_2} - \hat{t}_{cpa_1}) \sin(\theta)]^2$$

and finally

$$\tan(\hat{\theta}_f) = \frac{(\hat{\alpha}_1 - \hat{\alpha}_2)}{(\hat{t}_{cpa_2} - \hat{t}_{cpa_1})} \rightarrow \hat{v}_f = \frac{d \cos(\hat{\theta}_f)}{(\hat{t}_{cpa_2} - \hat{t}_{cpa_1})}. \quad (4.21)$$

It is important now to remark that these expressions of  $\hat{\theta}_f$  and  $\hat{v}_f$  as given by (4.21) ensure that  $F(\hat{v}_f, \hat{\theta}_f)$  is zero, which means that

$$\hat{\alpha}_2 = \hat{\alpha}_1 - \frac{d}{\hat{v}_f} \sin(\hat{\theta}_f), \quad \hat{t}_{cpa_2} = \hat{t}_{cpa_1} + \frac{d}{\hat{v}_f} \cos(\hat{\theta}_f). \quad (4.22)$$

Thus, it is legitimate (for this fusion rule) to consider a definition of distance between the two tracklets  $\hat{\mathbf{Y}}_1$  and  $\hat{\mathbf{Y}}_2$  as

$$d(\hat{\mathbf{Y}}_1, \hat{\mathbf{Y}}_2) = \max\{|\hat{\theta}_f - \hat{\theta}_2|, |\hat{\theta}_f - \hat{\theta}_1|\}, \quad (4.23)$$

$\hat{\theta}_f$  being given by Eq. (4.21). As we will see the interest of this distance is that it is close to the optimal one (see Section 4.4), while the non-centrality parameter is now made explicit.

To give credit to this assertion let us examine now the performance of this fused estimator (see Eqs. (4.21) and (4.22)), under the hypothesis of *valid association*.

$$\hat{\theta}_f = \arctan \left[ \frac{(\hat{\alpha}_1 - \hat{\alpha}_2)}{(\hat{t}_{cpa_2} - \hat{t}_{cpa_1})} \right]$$

$$\rightarrow \hat{v}_f = \frac{d \cos(\hat{\theta}_f)}{(\hat{t}_{cpa_2} - \hat{t}_{cpa_1})} \rightarrow \widehat{cpa}_1 = \frac{\hat{\alpha}_1}{\hat{v}_f}, (\hat{t}_{cpa_1}). \quad (4.24)$$

Immediate calculations yield

$$\hat{v}_f \stackrel{1}{=} v + \frac{v^2}{d} \cos(\theta) \varepsilon(t_{cpa_2} - t_{cpa_1}) + \frac{v^2}{d} \sin(\theta) \varepsilon(\alpha_1 - \alpha_2),$$

$$\hat{\theta}_f \stackrel{1}{=} \theta + \frac{v}{d} \sin(\theta) \varepsilon(t_{cpa_2} - t_{cpa_1}) - \frac{v}{d} \cos(\theta) \varepsilon(\alpha_1 - \alpha_2),$$

$$\widehat{cpa}_1 \stackrel{1}{=} cpa_1 + \left( v + \frac{vcpa_1}{d} \sin \theta \right) \varepsilon(\alpha_1) - \frac{vcpa_1}{d} \sin(\theta) \varepsilon(\alpha_2) + \left( \frac{vcpa_1}{d} \cos \theta \right) \varepsilon(t_{cpa_2} - t_{cpa_1}),$$

where  $v_f = v$  and  $\theta_f = \theta$ . (4.25)

Under the (asymptotic) Gaussian assumption the fused  $\hat{\mathbf{X}}_f$  estimator then has the following asymptotic distribution:

$$\begin{pmatrix} \widehat{cpa}_{1f} = \hat{\alpha}_1 \hat{v}_f \\ \hat{v}_f \\ \hat{\theta}_f \\ \hat{t}_{cpa_1} \end{pmatrix} \rightarrow \mathcal{N}(\mathbf{X}, MGM^T),$$

where

$$M = \begin{pmatrix} v \left( 1 + \frac{cpa_1}{d} \sin \theta \right) & -\frac{vcpa_1 \cos \theta}{d} & -\frac{vcpa_1 \sin \theta}{d} & \frac{vcpa_1 \cos \theta}{d} \\ \frac{v^2}{d} \sin \theta & -\frac{v^2}{d} \cos \theta & -\frac{v^2}{d} \sin \theta & \frac{v^2}{d} \cos \theta \\ -\frac{v}{d} \cos \theta & -\frac{v}{d} \sin \theta & \frac{v}{d} \cos \theta & \frac{v}{d} \sin \theta \\ 0 & 1 & 0 & 0 \end{pmatrix}$$

$\uparrow \qquad \qquad \uparrow \qquad \qquad \uparrow \qquad \qquad \uparrow$   
 $\varepsilon(\alpha_1) \qquad \varepsilon(t_{cpa_1}) \qquad \varepsilon(\alpha_2) \qquad \varepsilon(t_{cpa_2})$

(4.26)

$$G = \text{Cov}(\hat{\alpha}_1, \hat{t}_{cpa_1}, \hat{\alpha}_2, \hat{t}_{cpa_2}).$$

Again, it is quite insightful to calculate the volume of uncertainty associated with  $\hat{\mathbf{X}}_f$ , yielding

$$\det(MGM^T) = a^2 b^2 \frac{v^8}{d^4},$$

with  $\text{var}(\hat{\alpha}_1) = a$ ,  $\text{var}(\hat{t}_{cpa_1}) = b$ , (4.27)

which, compared with the performance of the optimal fusion rule (see Proposition 3) shows that this fusion rule is close to optimality, as far as the ratio *target speed/intersensor distance* is not too great. This justifies the use of the distance  $d(\hat{\mathbf{Y}}_1, \hat{\mathbf{Y}}_2)$  as given by Eq. (4.23).

### 4.4. The optimal fusion rule and its performance

Let us turn now toward the optimal fusion rule. The whole target state vector  $\hat{\mathbf{X}}$  is obtained as the solution of the following optimization problem:

$$\hat{\mathbf{X}}_{\text{opt}} \in \arg \min_{\mathbf{X}} \left\{ \|\hat{\mathbf{Y}}_1 - \mathbf{Y}_1(\mathbf{X})\|_{\Gamma_1^{-1}}^2 + \|\hat{\mathbf{Y}}_2 - \mathbf{Y}_2(\mathbf{X})\|_{\Gamma_2^{-1}}^2 \right\}. \quad (4.28)$$

Considering the above likelihood functional Eq. (4.28) as a  $\mathbf{X}$  one, its gradient vector is

$$-J_{\mathbf{X}}(\mathbf{Y}_1(\mathbf{X}))\Gamma_1^{-1}(\hat{\mathbf{Y}}_1 - \mathbf{Y}_1(\mathbf{X})) - J_{\mathbf{X}}(\mathbf{Y}_2(\mathbf{X}))\Gamma_2^{-1}(\hat{\mathbf{Y}}_2 - \mathbf{Y}_2(\mathbf{X})),$$

where

$$J_{\mathbf{X}}(\mathbf{Y}_1(\mathbf{X})) = \begin{pmatrix} \frac{1}{v} & 0 & 0 \\ \frac{-cpa_1}{v^2} & 0 & 0 \\ 0 & 1 & 0 \\ 0 & 0 & 1 \end{pmatrix},$$

$$J_{\mathbf{X}}(\mathbf{Y}_2(\mathbf{X})) = \begin{pmatrix} \frac{1}{v} & 0 & 0 \\ \frac{d \sin(\theta) - cpa_1}{v^2} & 0 & -\frac{d}{v^2} \cos(\theta) \\ -\frac{d}{v} \cos(\theta) & 1 & -\frac{d}{v} \sin(\theta) \\ 0 & 0 & 1 \end{pmatrix}. \quad (4.29)$$

Assuming the  $\hat{\mathbf{Y}}_1$  and  $\hat{\mathbf{Y}}_2$  tracklets<sup>7</sup> uncorrelated, a classical calculation then yields the expression of the Fisher information matrix (FIM) associated with  $\hat{\mathbf{X}}_{\text{opt}}$  (Eq. (4.28)):

$$\text{FIM}_{\mathbf{X}}(\mathbf{Y}_1, \mathbf{Y}_2) = J_{\mathbf{X}}(\mathbf{Y}_1(\mathbf{X}))\Gamma_1^{-1}(J_{\mathbf{X}}(\mathbf{Y}_1(\mathbf{X})))^T + J_{\mathbf{X}}(\mathbf{Y}_2(\mathbf{X}))\Gamma_2^{-1}(J_{\mathbf{X}}(\mathbf{Y}_2(\mathbf{X})))^T. \quad (4.30)$$

It can be shown that the covariance of  $\hat{\mathbf{X}}_{\text{opt}}$  ( $\text{cov}(\hat{\mathbf{X}}_{\text{opt}})$ ) asymptotically tends toward the inverse of the  $\text{fim}_{\mathbf{X}}$  matrix, so that (see Appendix C):

**Proposition 3.** *Asymptotically, the uncertainty volume related to the optimal fusion rule is given by*

$$\det(\text{cov}(\hat{\mathbf{X}}_{\text{opt}})) \rightarrow (\det(\text{FIM}_{\hat{\mathbf{X}}_{\text{opt}}}))^{-1} = \psi(\Gamma, v, d),$$

where the functional  $\psi(\Gamma, v, d)$  is given by

$$\Gamma^{-1} = \text{diag}(a, b, c) \rightarrow \psi(\Gamma, v, d) = \frac{v^8}{acd^2 [acd^2 + 2ab(1 - 2\cos(2\theta))v^2 + 2bc(1 + 2\cos(2\theta))v^2]},$$

$$\Gamma^{-1} = ald \rightarrow \psi(\Gamma, v, d) = \frac{1}{a^4} \frac{v^8}{[d^2(4v^2 + a^2d^2)]}. \quad (4.31)$$

Thus, it has been shown that the volume of uncertainty is this time  $\left(\frac{1}{a^4} \frac{v^8}{[d^2(4v^2 + a^2d^2)]}\right)$  ( $\Gamma^{-1} = ald$ ). Moreover, we see that in the general case  $\Gamma = \text{diag}(a, b, c)$  the effects of the signal processing performance on the one hand and of the target-receivers geometry on the other cannot be separated.

<sup>7</sup>  $\hat{\mathbf{Y}}_1$  represent a partial estimation of the complete target state, hence the name “tracklet”.

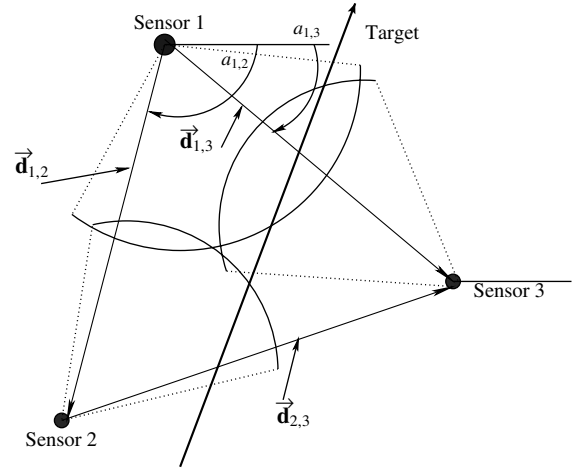


Fig. 6. A target crossing a triangle network.

Maximizing the likelihood functional requires an iterative method. Clearly, if the unique track assumption is valid, the previous approaches are quite convenient for initializing it, while convergence is investigated in Appendix D. In this appendix, it is shown that an iterative algorithm would converge toward the exact solution, under the *common track* assumption.

Usually, the basic element of a sensor network is made of three sensors forming a triangle. Thus, it is of a fundamental practical importance to analyze the performance of (optimal) fusion for such configuration. The geometry and the definitions of the various parameters are depicted in Fig. 6 ( $a_{1,2} = (\vec{i}, \vec{d}_{1,2})$ ,  $d_{1,2} = \|\vec{d}_{1,2}\|$ ).

Elementary calculations yield (see Fig. 6)

$$t_{cpa_2} = t_{cpa_1} + \frac{d_{1,2}}{v} \cos(\theta - a_{1,2}),$$

$$t_{cpa_3} = t_{cpa_1} + \frac{d_{1,3}}{v} \cos(\theta - a_{1,3}), \quad (4.32)$$

$$\alpha_2 = \alpha_1 - \frac{d_{1,2}}{v} \sin(\theta - a_{1,2}),$$

$$\alpha_3 = \alpha_1 - \frac{d_{1,3}}{v} \sin(\theta - a_{1,3}).$$

Taking sensor 1 as the reference, the Fisher information matrix is given by the sum  $\sum_{i=1}^3 J_{\mathbf{X}}(\mathbf{Y}_i(\mathbf{X}))J_{\mathbf{X}}^T(\mathbf{Y}_i(\mathbf{X}))$ , and the following result is shown in Appendix C:

$$\det(\text{FIM}) = \frac{d_{1,2}^2 d_{1,3}^2}{v^8} (1 + 3\cos^2(a_{1,2} - a_{1,3}))$$

$$+ 6 \left( \frac{d_{1,2}^2 + d_{1,3}^2}{v^6} \right) + \frac{\cos^2(\theta - a_{1,2})}{v^6} (d_{1,2}^2)$$

$$- \frac{\sin^2(\theta - a_{1,3})}{v^6} (d_{1,3}^2). \quad (4.33)$$

The result we have obtained is in the same vein than that of Proposition 3. Concerning the  $d^4/v^8$  term, there is a

Table 1  
Comparison of the performance of various fusion rules

Fusion rule	Uncertainty volume for $\hat{\mathbf{X}}$	Simplified expression	Optimization
Fusion of the ( <i>cpa/v</i> ) ratios	$\varphi(\Gamma) \left[ \frac{(\sigma_1^4 + \sigma_2^4)v^4}{(\alpha_1 - \alpha_2)^2(\sigma_1^2 + \sigma_2^2)^2} \right]$	$\frac{v^6}{4d^2 \sin^2(\theta)}$	None Biased
Fusion of the $t_{cpa}$	$\varphi(\Gamma) \left[ \frac{(\sigma_1^4 + \sigma_2^4)v^4}{(t_{cpa1} - t_{cpa2})^2(\sigma_1^2 + \sigma_2^2)^2} \right]$	$\frac{v^6}{4d^2 \cos^2(\theta)}$	None Biased
Optimal fusion rule	$\frac{v^8}{a^4 d^2 [a^2 d^2 + 4v^2]} (\Gamma^{-1} = aId)$	$\frac{v^8}{(4d^2 v^2 + a^2 d^4)}$	Iterative Asympt. Unbiased
Track association fusion rule	$a^2 b^2 \frac{v^8}{d^4}$	$\frac{v^8}{d^4}$	None Biased

neat improvement due to the network since the factor of this term is now  $(1 + 3 \cos^2(a_{1,2} - a_{1,3}))$  (instead of 1). A similar remark for the  $d^2/v^6$  term can be made. The interest of considering the three sensors as an elementary network is thus evident. Finally, Propositions 1 and 2 (*cpa* and  $t_{cpa}$  fusion rules can be extended to a network of an arbitrary geometry.

Effect of tracklet correlation can be analyzed in the same way. Actually, tracklet correlation may occur if the temporal support for signal processing are not disjoint (see Fig. 6). This is tightly related to the intersensor distance, target velocity, integration time, etc. In this case, Eq. (4.30) is replaced by the following one:

$$\begin{aligned} \text{FIM}_{\mathbf{X}}(\mathbf{Y}_1, \mathbf{Y}_2) &= (J_{\mathbf{X}}(\mathbf{Y}_1(\mathbf{X})), J_{\mathbf{X}}(\mathbf{Y}_2(\mathbf{X}))) \\ &\times \begin{pmatrix} \Gamma_1^{-1} & \text{Cor}^{-1} \\ \text{Cor}^{-1} & \Gamma_2^{-1} \end{pmatrix} \begin{pmatrix} J_{\mathbf{X}}^T(\mathbf{Y}_1(\mathbf{X})) \\ J_{\mathbf{X}}^T(\mathbf{Y}_2(\mathbf{X})) \end{pmatrix}. \end{aligned} \quad (4.34)$$

Then, under the assumptions  $\Gamma^{-1} = aId$ , and  $(\text{Cor})^{-1} = \text{cor}Id$ , the  $\psi(\Gamma, v, d)$  functional (see Proposition 3) is replaced by

$$\psi(\Gamma, \text{Cor}, v, d) = \frac{v^8}{(a^2 - \text{cor}^2)^2 d^2 [(a^2 - \text{cor}^2)d^2 + 4v^2]}. \quad (4.35)$$

#### 4.5. Selecting the fusion rule

It has been shown that the *cpa* fusion rule has to be rejected when target heading is close to  $0^\circ$  (modulo  $\pi$ ) whereas the  $t_{cpa}$  is clearly irrelevant for target headings close to  $90^\circ$  (modulo  $\pi$ ). Between these two extreme cases, the best way to select the right fusion rule is to calculate their respective performance. For the sake of clarity, the previous results are summarized in Table 1.

While the use of the optimal fusion rule requires iterative methods, they can be initialized via the non-iterative ones. Furthermore, it is wise to test the validity

of tracklet association (see the track association fusion rule) before performing a finer estimation. Thus, these four methods are not really concurrent. The best way is certainly to combine them.

#### 4.6. Simulations

To illustrate the benefits of decentralized estimation, we shall consider the framework of Section 2. For Monte Carlo simulations (500 runs), two sensors separated by a distance of 800 m are considered with a target going through the array with a heading equal to  $90^\circ$  and a distance of *cpa* relatively to sensor 1 equal to 300 m. Its velocity is 5 m/s, its electric moment is 50 A m and electric noises on the axes of both sensors have a variance equal to  $200 \text{ nV}^2/\text{m}^2$ . On Fig. 7 (top), we can see the collected signals and the histograms of the estimated parameters (via decentralized processing<sup>8</sup>) as well as their theoretical PDF (prob. density function) and centralized processing PDF.<sup>9</sup>

Considering Fig. 7, we can conclude that the behaviour of the fused estimators agrees with the theoretical performance and is close to optimality. The advantages of decentralized estimation are evident for practical applications.

### 5. Track-to-track association

Up to now, the problem was to estimate the target motion parameters. However, another question is to decide if a unique target is present or not. Consider the case where multiple detections arise in the network. Is there is *one* target crossing the network, or *more*? An answer to this question cannot be given by a short time

<sup>8</sup> Decentralized processing means here that  $\hat{\mathbf{X}}$  is estimated via the *cpa/v* fusion rule of the  $\hat{\mathbf{Y}}_i$  tracklets.

<sup>9</sup> Centralized means here that the target motion parameters are estimated via centralized signal processing.

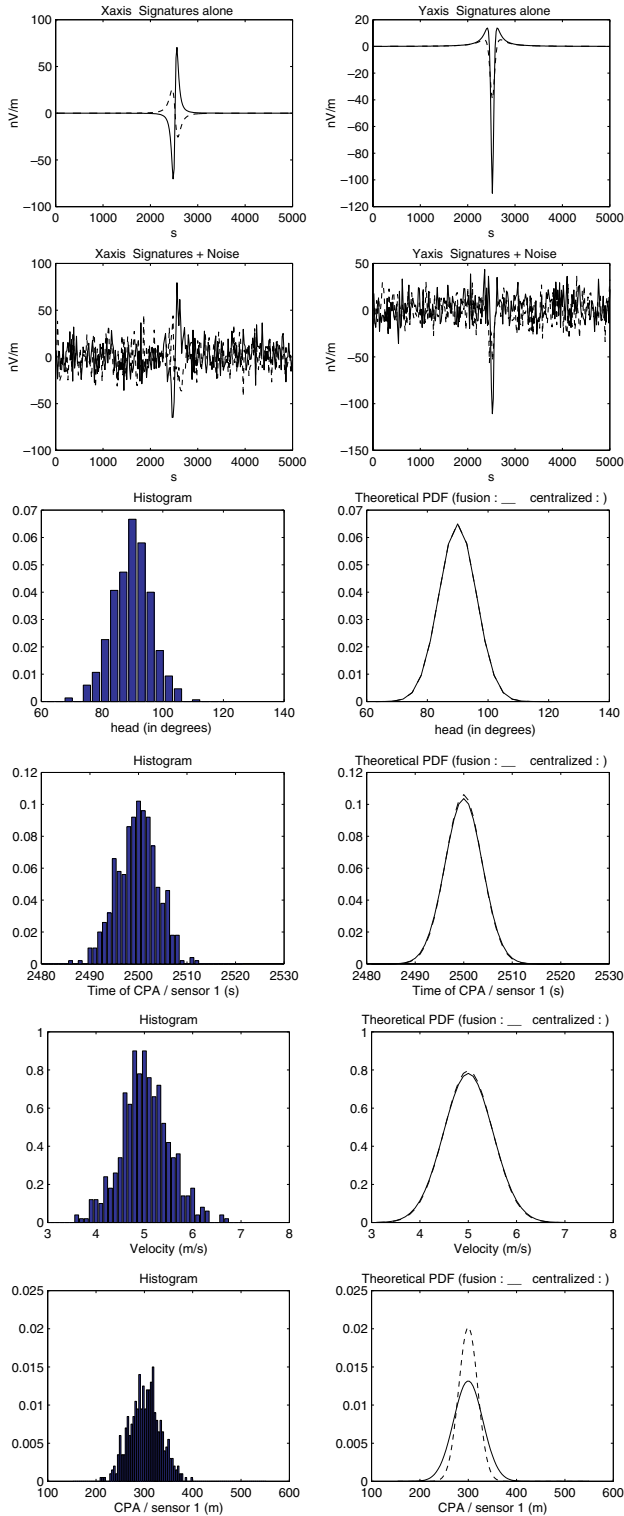


Fig. 7. Simulation results. Top: theoretical and noised UEP signatures of a moving target. Middle and bottom: right: theoretical PDF of fused and centralized estimates of the kinematic target vector components (4), left: histograms of the estimates.

analysis, so it must be based on spatio-temporal processing. Again, for the sake of brevity, we assume that we have two sensors, each one estimating one tracklet can-

didate. This study will be divided in two parts. The first one is devoted to the valid association hypothesis; while the second precisely investigates the validity of this assumption.

### 5.1. Valid association assumption

The idea, inspired by [13], consists in testing the association of two (partial) tracklets. The corresponding scenario is represented on Fig. 2. Let  $\hat{\mathbf{Y}}_1$  and  $\hat{\mathbf{Y}}_2$ , the vectors of (partial) estimates associated with sensor 1 and 2. We assume that these two vectors are normally distributed. More precisely,

$$\hat{\mathbf{Y}}_1 \rightarrow \mathcal{N}(\mathbf{Y}_1, \Gamma_1), \quad \hat{\mathbf{Y}}_2 \rightarrow \mathcal{N}(\mathbf{Y}_2, \Gamma_2), \quad (5.1)$$

$$\hat{\mathbf{Y}}_1 = (\hat{\alpha}_1, \hat{\theta}_1, \hat{t}_{cpa_1})^T, \quad \hat{\mathbf{Y}}_2 = (\hat{\alpha}_2, \hat{\theta}_2, \hat{t}_{cpa_2})^T.$$

Invoking the deterministic relations Eq. (2.8), we shall test the proximity of the two vectors  $\hat{\mathbf{Y}}_2$  and  $\hat{\mathbf{Y}}_{1,2}$ , where  $\hat{\mathbf{Y}}_{1,2}$  is an updated version (on sensor 2) of  $\hat{\mathbf{Y}}_1$ , given by

$$\hat{\mathbf{Y}}_{1,2} = \left( \hat{\alpha}_1 - \frac{d}{v} \sin(\hat{\theta}_1), \hat{\theta}_1, \hat{t}_{cpa_1} + \frac{d}{v} \cos(\hat{\theta}_1) \right)^T. \quad (5.2)$$

Under the hypothesis of moderate estimation errors and denoting “ $\delta(\text{estimator})$ ” the error affecting the estimator, the following first-order expansions are considered:

$$\begin{aligned} \hat{\alpha}_1 - \frac{d}{v} \sin(\hat{\theta}_1) &\stackrel{1}{=} \alpha_1 - \frac{d}{v} \sin(\theta) + \delta(\hat{\alpha}_1) - \frac{d}{v} \cos(\theta) \delta(\hat{\theta}_1) \\ &\stackrel{1}{=} \alpha_2 + \delta(\hat{\alpha}_1) - \frac{d}{v} \cos(\theta) \delta(\hat{\theta}_1), \\ \hat{t}_{cpa_1} + \frac{d}{v} \cos(\hat{\theta}_1) &\stackrel{1}{=} t_{cpa_1} + \frac{d}{v} \cos(\theta) + \delta(\hat{t}_{cpa_1}) - \frac{d}{v} \sin(\theta) \delta(\hat{\theta}_1), \\ &\stackrel{1}{=} t_{cpa_2} + \delta(\hat{t}_{cpa_1}) - \frac{d}{v} \sin(\theta) \delta(\hat{\theta}_1). \end{aligned}$$

Consequently, under the assumption that the two sensors observe the same target, there is a value of the velocity  $v$  such that  $\hat{\mathbf{Y}}_{1,2}$  has the following distribution:

$$\hat{\mathbf{Y}}_{1,2} \rightarrow \mathcal{N}(\mathbf{Y}_2, J_{1,2}(v) \Gamma_1 J_{1,2}^T(v)),$$

where

$$J_{1,2}(v) = \begin{pmatrix} 1 & -\frac{d}{v} \cos(\theta) & 0 \\ 0 & 1 & 0 \\ 0 & -\frac{d}{v} \sin(\theta) & 1 \end{pmatrix}. \quad (5.3)$$

This means that the difference vector  $\Delta \hat{\mathbf{Y}}_{1,2}(v)$  ( $\Delta \hat{\mathbf{Y}}_{1,2}(v) = \hat{\mathbf{Y}}_2 - \hat{\mathbf{Y}}_{1,2}(v)$ ) is normal, centered and with a covariance matrix  $\Gamma(v)$  (given by  $\Gamma(v) = J_{1,2}(v) \Gamma_1 J_{1,2}^T(v) + \Gamma_2$ ). This value  $\hat{v}_{opt}$  of the target velocity is estimated by maximizing the likelihood function of the difference vector  $\Delta \hat{\mathbf{Y}}_{1,2}(v)$ . In this meaning, it is then defined by

$$\hat{v} \in \underset{v}{\operatorname{argmin}} \left[ \underbrace{\Delta \hat{\mathbf{Y}}_{1,2}(v)^T \Gamma^{-1}(v) \Delta \hat{\mathbf{Y}}_{1,2}(v)}_{F(v)} + \ln(2\pi \det(\Gamma(v))) \right]. \quad (5.4)$$

Let us consider the random variable  $F(\hat{v})$ . Practically, the matrix  $\Gamma(v)$  is unknown, so that it is replaced by an estimated matrix  $\hat{\Gamma}(v) = \hat{J}_{1,2}(v) \hat{\Gamma}_1 \hat{J}_{1,2}^T(v) + \hat{\Gamma}_2$ , with

$$\hat{J}_{1,2}(v) = \begin{pmatrix} 1 & -\frac{d}{v} \cos(\hat{\theta}) & 0 \\ 0 & 1 & 0 \\ 0 & -\frac{d}{v} \sin(\hat{\theta}) & 1 \end{pmatrix}, \quad \hat{\theta}_f = \frac{1}{\sigma_{\hat{\theta}_1}^2 + \sigma_{\hat{\theta}_2}^2} (\sigma_{\hat{\theta}_2}^2 \hat{\theta}_1 + \sigma_{\hat{\theta}_1}^2 \hat{\theta}_2). \quad (5.5)$$

Now, it can be shown that the random variable  $F(\hat{v})$  is asymptotically Chi-square distributed, with 3 degrees of freedom. Then, the decision (track association) is made on the basis of comparing  $F(\hat{v})$  with a threshold so as the probability to associate 2 tracks generated by a unique target be equal to a fixed level (e.g. 0.9), yielding the following test.

*Test.* The two tracks correspond to a unique target—with probability  $\beta$ —if  $F(\hat{v}) < \eta$ , with  $\eta$  defined by  $\int_0^\eta \chi_3^2(x) dx = \beta$ .

Before evaluating the performance of the method, it is worth noting that our system is passive and that some characters required in the calculation of the covariance matrix have to be estimated (namely:  $\hat{\theta}$  and  $\hat{\Gamma}_1, \hat{\Gamma}_2$ ). The following formula [9] is particularly useful for approximating the probability of correct association, denoted  $P_{CAS}$ :

$$\Pr[\chi_3^2 \leq x] = \frac{2(1/2x)^{3/2}}{\Gamma(3/2)} \sum_{j=0}^{\infty} (-1)^j \frac{x^j}{(3+2j)2^j j!}. \quad (5.6)$$

Note that the series above converges for all  $x > 0$  and, for sufficiently large  $m$ , the true value lies between  $\sum_{j=0}^m$  and  $\sum_{j=0}^{m+1}$  (alternate series). Practically, these two bounds can be used for fitting the value of the  $\eta$  parameter so as to have an appropriate value of  $P_{CAS}$ .

However, the main problem remains the calculation of the probability of false association ( $P_{FAS}$ ); i.e. the probability that two tracks be *falsely associated*. Following the above guideline, the problem is “classically” treated in the literature [7,21] by considering a non-central  $\chi_3^2(m)$  for the density of  $\Pr(\tilde{F}(\hat{v}))$ , where the non-centrality parameter  $m$  corresponds to the difference  $\Delta \hat{\mathbf{Y}}_{1,2}(v)$ . Approximations of  $\Pr(\chi_3^2(m) < \eta)$  are summarized and *conveniently* referenced in the statistical literature (see [9]). Unfortunately, this modelling of the false association is highly criticable.

First, the equality  $\Gamma = J_{1,2}(v) \Gamma_1 J_{1,2}^T(v) + \Gamma_2$  has no real statistical meaning if the unique target assumption is no longer valid. Second and more importantly, the estimated  $\hat{v}$  (see (5.4)) no longer corresponds to the hypothesis of a common track and the above development is simply irrelevant.

### 5.2. Validity of the unique target assumption

The previous section gives a quite satisfactory framework for testing the tracklet association and calculate its performance under the assumption that both tracklets belong to the same target track. The question we deal with here is to test the validity of this assumption. It is for that reason that we turn now toward the track association rule. The following test will then be considered (see Eq. (4.23)):

$$d(\hat{\mathbf{Y}}_1, \hat{\mathbf{Y}}_2) = \max\{|\hat{\theta}_f - \hat{\theta}_2|, |\hat{\theta}_f - \hat{\theta}_1|\} \leq \eta, \quad \tan(\hat{\theta}_f) = \frac{(\hat{\alpha}_1 - \hat{\alpha}_2)}{(\hat{t}_{cpa2} - \hat{t}_{cpa1})}. \quad (5.7)$$

It remains to approximate the density of  $d(\hat{\mathbf{Y}}_1, \hat{\mathbf{Y}}_2)$ . A first way is to consider that the difference  $\hat{\theta}_f - \theta_1$  is asymptotically Gaussian. Under this assumption, previous calculations yield

$$(\hat{\theta}_f - \theta_1) \rightarrow \mathcal{N}\left((\theta_f - \theta_1), 4\left(\frac{v}{d}\right)^2 \sin^2(\theta)\right), \quad \theta_f = \arctan\left(\frac{\alpha_1 - \alpha_2}{t_{cpa2} - t_{cpa1}}\right). \quad (5.8)$$

The scalar  $\frac{1}{4\left(\frac{v}{d}\right)^2 \sin^2(\theta)} (\hat{\theta}_f - \theta_1)^2$  is then asymptotically distributed as a  $\chi^2((\theta_f - \theta_1), 1)$ .

However, this approximation makes sense only under the valid association assumption. If not, the problem can be considered in the two following ways. A first one is based on simulation methods; e.g. bootstrapping this density. For the sake of brevity, this approach will not be detailed here. Another approach is more explicit. From the definition of  $\tan(\hat{\theta}_f)$  (see Eq. (5.7)) we note that it is the ratio of two normal quantities, it is precisely

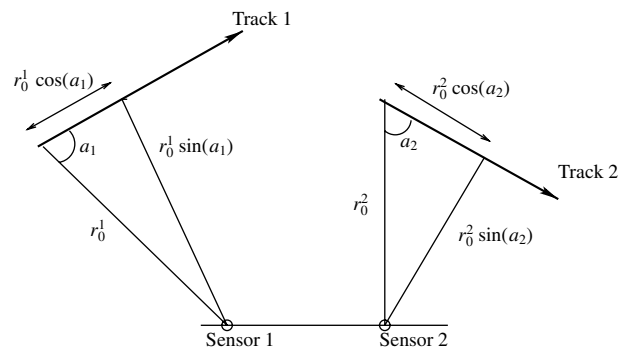


Fig. 8. A geometric interpretation of  $\theta_f$ .

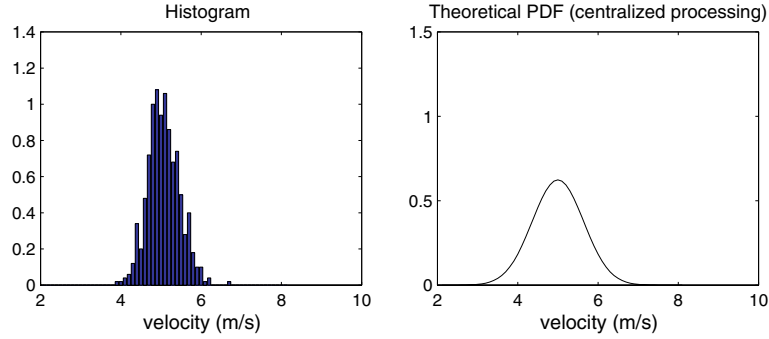


Fig. 9. Simulations results. Theoretical PDF (right) and histogram (left) of  $\hat{v}$  (see (5.4)).

the aim of Appendix F to provide a convenient expression of the distribution of  $\tan(\hat{\theta}_f)$ , given by Eq. (5.7). Even if calculations seem rather complicated, calculating the  $P_{FAS}$  is quite feasible by this way.

Let us now consider a more intuitive meaning of  $\tan(\hat{\theta}_f)$  (see Eq. (5.7)). Denoting  $a_1$  (respectively,  $a_2$ ) the  $(\vec{x}_0^1, \vec{v}_1)$  angle (resp.  $(\vec{x}_0^2, \vec{v}_2)$  angle), the angle  $\theta_f$  has the following interpretation (see Appendix A and Fig. 8):

$$\tan(\theta_f) = \frac{\begin{vmatrix} r_0^1 \sin a_1 & v_1 \\ r_0^2 \sin a_2 & v_2 \end{vmatrix}}{\begin{vmatrix} r_0^1 \cos a_1 & v_1 \\ r_0^2 \cos a_2 & v_2 \end{vmatrix}} = \frac{\begin{vmatrix} |\vec{x}_0^1, \vec{v}_1| & \langle \vec{v}_1, \vec{v}_1 \rangle \\ |\vec{x}_0^2, \vec{v}_2| & \langle \vec{v}_2, \vec{v}_2 \rangle \end{vmatrix}}{\begin{vmatrix} \langle \vec{x}_0^1, \vec{v}_1 \rangle & \langle \vec{v}_1, \vec{v}_1 \rangle \\ \langle \vec{x}_0^2, \vec{v}_2 \rangle & \langle \vec{v}_2, \vec{v}_2 \rangle \end{vmatrix}}. \quad (5.9)$$

Practically, a distance between two tracks can be defined by

$$d(\mathbf{X}_1, \mathbf{X}_2) = \frac{1}{T+1} \sum_{t=0}^T \|\mathbf{x}_0^1 - \mathbf{x}_0^2 + t(v_1 - v_2)\|^2 \quad (5.10)$$

and for which a value of  $\tan(\theta_f)$  is given by (5.9).

The whole algorithm for tracklet association then takes the following form:

#### Tracklet association algorithm

1. Check the validity of the unique target assumption (see Section 5.2),
2. Unique target  $\rightarrow$  perform the tracklet association test (see Section 5.1).

#### 5.3. Simulation results

We present on Fig. 9 the signatures collected on each sensor for a target going across the array, at a distance of 400 m from each sensor and having the characteristics of the target simulated in the previous chapter. Using 500 runs of this scenario, the velocity histogram has been computed and compared with the corresponding theoretical PDF given by the centralized processing.

On these 500 trials, the empirical estimate of the probability of association has been found equal to

0.907, which is very close to the theoretical values (0.9). The same agreement holds for the velocity estimator. Its performance seems even better than the theoretical performance of the (optimal) centralized processing. Small differences may be due to: the trial number (here 500); the exact values of missing parameters (here the target heading and the sensor covariance matrix) are replaced by their estimates, the errors incoming from these estimates can partially compensate errors inherent to the fusion method [13].

## 6. Conclusion

This paper deals with detection/motion analysis of a target crossing an array of sensors. Since the motion parameters are only partially estimated at the sensor level, various fusion rules have been considered and their performance analyzed in a general framework based on multilinear algebra. Then the track-to-track association problem is examined, as well as the associated testing and their performance. In particular, it is shown that decentralized processing is close to optimality while being intrinsically robust, a definite advantage. Moreover, performance analysis allows to quantify the effects of the various components of the detection system at a fusion level.

## Acknowledgements

The authors are grateful to the referees for their many helpful comments and to the editor for an insightful review process.

## Appendix A. From Cartesian to CPA coordinates

The sensor is located at the origin  $O$ . The target starts from the  $M_0$  point and follows a rectilinear and uniform motion ( $\vec{v}$ ). Then, the CPA point  $M_{cpa}$  is characterized by:

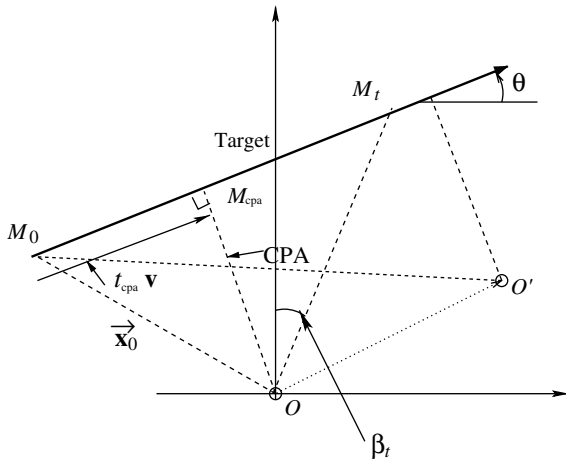


Fig. 10. From Cartesian to CPA coordinates.

the vectors  $\overrightarrow{OM_{cpa}}$  ( $OM_0 = \vec{x}_0$ ) and  $\overrightarrow{M_0M_{cpa}}$  are orthogonal, so that we have (see Fig. 10)

$$(x_0 + t_{cpa}v_x)v_x + (y_0 + t_{cpa}v_y)v_y = 0 \quad (t_{cpa} \neq 0),$$

so that

$$t_{cpa} = -\frac{\langle \vec{x}_0, \vec{v} \rangle}{\|\vec{v}\|^2} = -\frac{r_0}{v} \cos(\vec{x}_0, \vec{v}). \tag{A.1}$$

Similarly, we obtain the following expression of  $cpa \triangleq \|\overrightarrow{OM_{cpa}}\|$ :

$$\begin{aligned} \|\overrightarrow{OM_{cpa}}\| &= [(x_0 + t_{cpa}v_x)^2 + (y_0 + t_{cpa}v_y)^2]^{1/2}, \\ &= \left[ \|\vec{x}_0\|^2 - \frac{\langle \vec{x}_0, \vec{v} \rangle^2}{\|\vec{v}\|^2} \right]^{1/2}, \\ &= \|\vec{x}_0\| |\sin(\vec{x}_0, \vec{v})| = \frac{|\det(\vec{x}_0, \vec{v})|}{v}. \end{aligned} \tag{A.2}$$

The 1:1 correspondence between Cartesian and CPA coordinates reads as follows:

$$\begin{pmatrix} \vec{x}_0 \\ \vec{v} \end{pmatrix} \rightarrow \begin{pmatrix} |\det(\vec{x}_0, \vec{v})| \\ \langle \vec{x}_0, \vec{v} \rangle \\ \theta \\ v \end{pmatrix} \rightarrow \begin{pmatrix} \frac{|\det(\vec{x}_0, \vec{v})|}{v} = cpa \\ v \\ \theta \\ -\frac{\langle \vec{x}_0, \vec{v} \rangle}{\|\vec{v}\|^2} = t_{cpa} \end{pmatrix}. \tag{A.3}$$

Showing that it is a 1:1 transform is straightforward. Moreover, the following formulas are easily inferred from Eqs. (A.1) and (A.2)<sup>10</sup> and used throughout this text:

<sup>10</sup> For the second one we assume that  $\det(\vec{x}_0, \vec{v})$  and  $\det(\overrightarrow{OO'}, \vec{v})$  have the same sign.

$$t_{cpa_2} = \frac{\langle \overrightarrow{OO'}, \vec{v} \rangle}{v^2} + t_{cpa_1}, \tag{A.4}$$

$$cpa_2 = -\frac{\det(\overrightarrow{OO'}, \vec{v})}{v} + cpa_1.$$

More generally and with the notations of Fig. 10 ( $\beta_t$  being the target azimuth), we have

$$\begin{aligned} \overrightarrow{OM_t} &= \overrightarrow{OM_{cpa}} + \overrightarrow{M_{cpa}M_t} \quad \text{with} \\ M_{cpa} &= \begin{cases} -cpa \sin \theta \\ cpa \cos \theta \end{cases}, \quad \overrightarrow{M_{cpa}M_t} = (t - t_{cpa})\vec{v}, \end{aligned} \tag{A.5}$$

so that

$$\sin(\beta_t) = \frac{-\alpha \sin \theta + (t - t_{cpa}) \cos \theta}{\alpha \cos \theta + (t - t_{cpa}) \sin \theta}.$$

As an illustration, let us consider the temporal evolution of the frequency  $f_t$  of the received signal at the instant  $t$ , emitted by a moving target, which is given by

$$f(t) = f_0 \left( 1 - \frac{v_x}{c} \sin(\beta_t) - \frac{v_y}{c} \cos(\beta_t) \right), \tag{A.6}$$

$$v_x = v \cos(\theta), \quad v_y = v \sin(\theta), \tag{A.7}$$

where  $f_0$  is the initial target frequency,  $c$  is the wave celerity, and  $\sin(\beta_t)$  is given by Eq. (A.5). Again, from Eq. (A.5), it is clear that the observable parameters are  $\{\frac{cpa}{v}, t_{cpa}, \theta\}$ . Actually, it can be shown the observability of all the passive systems is related to the analysis of ( $\beta_t$ ) and its temporal derivatives [12].

### Appendix B. Performance of the CPA fusion rule

The aim of this Appendix is to give a proof of Property 1. The matrix  $\Gamma$  being positive definite, it may be factored in triangular factor (i.e.  $\Gamma = \mathcal{T} \mathcal{T}^T$ ), so that we have

$$M_1 \Gamma M_1^T + M_2 \Gamma M_2^T = \mathcal{M}_1 \mathcal{M}_1^T + \mathcal{M}_2 \mathcal{M}_2^T \tag{B.1}$$

$$= (\mathcal{M}_2 \mathcal{M}_1) (\mathcal{M}_2^T \mathcal{M}_1^T), \tag{B.2}$$

where  $\mathcal{M}_i \triangleq M_i \mathcal{T}$  ( $i = 1, 2$ ). The matrices  $\mathcal{M}_i$  are rectangular, here  $4 \times 3$ . To calculate the previous determinant (last row of Eq. (B.1)), the Binet–Cauchy formula [6] will be instrumental. Let us introduce the notation  $\mathcal{M}^i$  for the  $i$ th row of the rectangular concatenated matrix  $(\mathcal{M}_2 \quad \mathcal{M}_1)$  (here  $4 \times 6$ ).

Of course, a brute force calculation of this  $4 \times 4$  determinant calculation would be to first calculate the  $(\mathcal{M}_2 \quad \mathcal{M}_1) \begin{pmatrix} \mathcal{M}_2 \\ \mathcal{M}_1 \end{pmatrix}$  matrix and then its determinant.

But, no geometric insight is obtained by this way, which is furthermore quite limited. Indeed, the Binet formula is the natural framework for performing such calculation since it involves only calculation of elementary determinants and uses *basically* multilinear algebra. Using it and the previous notations, we obtain

$$\begin{aligned} & \det(M_1 \Gamma M_1^T + M_2 \Gamma M_2^T) \\ &= \sum_{1 \leq i_1 < i_2 < i_3 < i_4 \leq 6} [\det(\mathcal{M}^{i_1}, \mathcal{M}^{i_2}, \mathcal{M}^{i_3}, \mathcal{M}^{i_4})]^2, \end{aligned}$$

where the vector  $\mathcal{M}^{i_j}$  is a column of  $\mathcal{M}_1$  or  $\mathcal{M}_2$ .

(B.3)

Assume for a while that  $\Gamma$  is the identity matrix and let us consider the structure of  $\mathcal{M}_2$  and  $\mathcal{M}_1$ , we have from (4.8)

$$\mathcal{M}_2 = (\mathbf{M}_2^1, \mathbf{M}_2^2, \mathbf{0}), \quad \mathcal{M}_1 = (v \mathbf{E}_1 - \mathbf{M}_2^1, \mathbf{M}_2^2, \mathbf{E}_4), \quad (\text{B.4})$$

where  $\mathbf{M}_2^i$  denotes the  $i$ th column of the  $\mathcal{M}_2$  ( $\mathbf{M}_2^3 = \mathbf{0}$ ), and  $\mathbf{E}_1$  and  $\mathbf{E}_4$  are the first and fourth vectors of the canonical basis of  $\mathbb{R}^4$ . Thus, we have

$$(\mathcal{M}_2, \mathcal{M}_1) = (\mathbf{M}_2^1, \mathbf{M}_2^2, \mathbf{0}, v \mathbf{E}_1 - \mathbf{M}_2^1, \mathbf{M}_2^2, \mathbf{E}_4). \quad (\text{B.5})$$

Now, starting from the left of the  $(\mathcal{M}_2, \mathcal{M}_1)$  array and using the Binet [6] formula (see (B.3)), we obtain

$$\begin{aligned} & \sum_{1 \leq i_1 < i_2 < i_3 < i_4 \leq 6} [\det(\mathcal{M}^{i_1}, \mathcal{M}^{i_2}, \mathcal{M}^{i_3}, \mathcal{M}^{i_4})]^2 \\ &= [\det(\mathbf{M}_2^1, \mathbf{M}_2^2, v \mathbf{E}_1, \mathbf{E}_4)]^2. \end{aligned} \quad (\text{B.6})$$

This is simply due to the fact that all the terms  $\det(\mathcal{M}^{i_1}, \mathcal{M}^{i_2}, \mathcal{M}^{i_3}, \mathcal{M}^{i_4})$  are zero but one ( $\det(\mathbf{M}_2^1, \mathbf{M}_2^2, v \mathbf{E}_1, \mathbf{E}_4)$ ). Thus, we have

$$\det(\mathcal{M}_1 \mathcal{M}_1^T + \mathcal{M}_2 \mathcal{M}_2^T) = v^2 [\det(\mathbf{E}_1, \mathbf{M}_2^1, \mathbf{M}_2^2, \mathbf{E}_4)]^2, \quad (\text{B.7})$$

$$= \frac{1}{4} \frac{v^4}{(\alpha_1 - \alpha_2)^2}. \quad (\text{B.8})$$

Extending the previous calculation to the case where  $\Gamma = \text{diag}(a, b, c)$  is now rather easy. Indeed, we have  $\Gamma = \mathcal{T} \mathcal{T}^T$ , with  $\mathcal{T} = \text{diag}(\alpha, \beta, \gamma)$  ( $\alpha^2 = a, \beta^2 = b, \gamma^2 = c$ ), so that

$$(M_2 \mathcal{T}, M_1 \mathcal{T}) = (\alpha \mathbf{M}_2^1, \beta \mathbf{M}_2^2, \mathbf{0}, \alpha v \mathbf{E}_1 - \alpha \mathbf{M}_2^1, \beta \mathbf{M}_2^2, \gamma \mathbf{E}_4),$$

and finally

$$\begin{aligned} & \det(\mathcal{M}_1 \mathcal{M}_1^T + \mathcal{M}_2 \mathcal{M}_2^T) \\ &= (\alpha^2 \beta \gamma)^2 v^2 \times [\det(\mathbf{E}_1, \mathbf{M}_2^1, \mathbf{M}_2^2, \mathbf{E}_4)]^2 = \frac{1}{4} (a^2 b c) \frac{v^4}{(\alpha_1 - \alpha_2)^2}. \end{aligned} \quad (\text{B.9})$$

If the  $\Gamma_1$  and  $\Gamma_2$  matrices are still diagonal but dissimilar, the matrix  $(M_2 \mathcal{T}, M_1 \mathcal{T})$  is replaced by  $(M_2 \mathcal{T}_2, M_1 \mathcal{T}_1)$  ( $\mathcal{T}_2^2 = \text{diag}(a', b', c')$ ,  $\mathcal{T}_1^2 = \text{diag}(a, b, c)$ ):

$$(M_2 \mathcal{T}_2, M_1 \mathcal{T}_1) = (\alpha' \mathbf{M}_2^1, \beta' \mathbf{M}_2^2, \mathbf{0}, \alpha v \mathbf{E}_1 - \alpha \mathbf{M}_2^1, \beta \mathbf{M}_2^2, \gamma \mathbf{E}_4),$$

and finally

$$\begin{aligned} & \det(\mathcal{M}_1 \mathcal{M}_1^T + \mathcal{M}_2 \mathcal{M}_2^T) \\ &= 2 \left( a a' \frac{(b+b')}{2} c \right)^2 v^2 [\det(\mathbf{E}_1, \mathbf{M}_2^1, \mathbf{M}_2^2, \mathbf{E}_4)]^2. \end{aligned} \quad (\text{B.10})$$

Consider now a more general form of the Gamma matrix, i.e.  $\Gamma = \mathcal{T} \mathcal{T}^T$ , with

$$\mathcal{T} = \begin{pmatrix} \alpha & 0 & 0 \\ \beta & \alpha & 0 \\ \gamma & \beta & \alpha \end{pmatrix}, \quad (\text{B.11})$$

then

$$\begin{aligned} (M_2 \mathcal{T}, M_1 \mathcal{T}) &= (\alpha \mathbf{M}_2^1 + \beta \mathbf{M}_2^2, \alpha \mathbf{M}_2^2, \mathbf{0}; \alpha v \mathbf{E}_1 - \alpha \mathbf{M}_2^1 \\ &\quad + \beta \mathbf{M}_2^2 + \gamma \mathbf{E}_4, \alpha \mathbf{M}_2^2 + \beta \mathbf{E}_4, \alpha \mathbf{E}_4) \end{aligned}$$

and only the following subdeterminants are not zeroed:

$$\det(\alpha \mathbf{M}_2^1 + \beta \mathbf{M}_2^2, \alpha \mathbf{M}_2^2, \alpha v \mathbf{E}_1, \beta \mathbf{E}_4),$$

$$\det(\alpha \mathbf{M}_2^1 + \beta \mathbf{M}_2^2, \alpha \mathbf{M}_2^2, \alpha v \mathbf{E}_1, \alpha \mathbf{E}_4)$$

and again

$$\begin{aligned} & \det(\mathcal{M}_1 \mathcal{M}_1^T + \mathcal{M}_2 \mathcal{M}_2^T) \\ &= v^2 [\alpha^8 + \alpha^6 \beta^2] [\det(\mathbf{E}_1, \mathbf{M}_2^1, \mathbf{M}_2^2, \mathbf{E}_4)]^2. \end{aligned} \quad (\text{B.12})$$

Obviously, this calculation is valid for any factorization of the Gamma matrix. Extension to the case of dissimilar  $\Gamma_1$  and  $\Gamma_2$  matrices is also straightforward. More precisely, only the following subdeterminants have to be considered (see Eq. (B.12)):

$$\det(\alpha' \mathbf{M}_2^1 + \beta' \mathbf{M}_2^2, \alpha' \mathbf{M}_2^2, \alpha v \mathbf{E}_1, \beta \mathbf{E}_4),$$

$$\det(\alpha' \mathbf{M}_2^1 + \beta' \mathbf{M}_2^2, \alpha' \mathbf{M}_2^2, \alpha v \mathbf{E}_1, \alpha \mathbf{E}_4),$$

and again

$$\begin{aligned} & \det(\mathcal{M}_1 \mathcal{M}_1^T + \mathcal{M}_2 \mathcal{M}_2^T) \\ &= v^2 [\alpha'^4 \alpha^4 + \alpha'^4 \alpha^2 \beta^2] [\det(\mathbf{E}_1, \mathbf{M}_2^1, \mathbf{M}_2^2, \mathbf{E}_4)]^2. \end{aligned} \quad (\text{B.13})$$

The general case of a Toeplitz  $\Gamma$  matrix is treated in the same way.

### Appendix C. On the performance of the optimal fusion rule

With the notations of Section 4.4 and the guidelines of the previous Appendix, we have to consider the following concatenated matrix:

$$[J_X \mathbf{Y}_1(\mathbf{X}), J_X \mathbf{Y}_2(\mathbf{X})]$$

$$= [\mathbf{M}_1, \mathbf{E}_3, \mathbf{E}_4; \mathbf{M}_1 + \mathbf{M}_2, \mathbf{E}_3, \mathbf{E}_4 + \mathbf{N}_2],$$

where

$$\mathbf{M}_1 = \begin{pmatrix} \frac{1}{v} \\ -\frac{c p a_1}{v^2} \\ 0 \\ 0 \end{pmatrix}, \quad \mathbf{M}_2 = \begin{pmatrix} 0 \\ \frac{d \sin \theta}{v^2} \\ -\frac{d \cos \theta}{v} \\ 0 \end{pmatrix}, \quad \mathbf{N}_2 = \begin{pmatrix} 0 \\ -\frac{d \cos \theta}{v^2} \\ \frac{d \sin \theta}{v} \\ 0 \end{pmatrix}, \quad (\text{C.1})$$



We note in passing that the vectors  $\mathbf{M}_2$  and  $\mathbf{N}_2$  are orthogonal. Using again the Binet formula, the calculation of  $\det(\sum_{i=1}^2 J_{\mathbf{X}} \mathbf{Y}_i(\mathbf{X}) J_{\mathbf{X}} \mathbf{Y}_i(\mathbf{X})^T)$  simply reduces to the calculation of the following (sub) determinants:

$$\begin{aligned} \det(\mathbf{M}_1, \mathbf{E}_3, \mathbf{E}_4, \mathbf{M}_2) &= (d/v^3) \sin(\theta), \\ \det(\mathbf{M}_1, \mathbf{E}_3, \mathbf{E}_4, \mathbf{N}_2) &= (d/v^3) \cos(\theta), \\ \det(\mathbf{M}_1, \mathbf{M}_2, \mathbf{N}_2, \mathbf{E}_4) &= d^2/(v^4). \end{aligned} \quad (\text{C.2})$$

Collecting the previous calculations, we obtain

$$\begin{aligned} \det \left( \sum_{i=1}^2 J_{\mathbf{X}} \mathbf{Y}_i(\mathbf{X}) J_{\mathbf{X}} \mathbf{Y}_i(\mathbf{X})^T \right) &= [\det(\mathbf{M}_1, \mathbf{M}_2, \mathbf{N}_2, \mathbf{E}_4)]^2 \\ &\quad + 4[\det(\mathbf{M}_1, \mathbf{E}_3, \mathbf{E}_4, \mathbf{M}_2)]^2 \\ &\quad + 4[\det(\mathbf{M}_1, \mathbf{E}_3, \mathbf{E}_4, \mathbf{N}_2)]^2 \\ &= \frac{d^4}{v^8} + 4 \frac{d^2}{v^6}. \end{aligned} \quad (\text{C.3})$$

Considering all the preceding results, we note that from a performance analysis perspective, the effect of the optimal fusion versus the  $cpa$  or  $t_{cpa}$  fusion is

1. combine both optimally,
2. add the term  $[\det(\mathbf{M}_1, \mathbf{M}_2, \mathbf{N}_2, \mathbf{E}_4)]^2$ .

Consider now that we have  $n$  sensors on the same line (see Fig. 2), then

$$\begin{aligned} J_{\mathbf{X}} \mathbf{Y}_i(\mathbf{X}) &= (\mathbf{M}_1 + (i-1)\mathbf{M}_2, \mathbf{E}_3, \mathbf{E}_4 + (i-1)\mathbf{N}_2), \\ 2 &\leq i \leq n. \end{aligned} \quad (\text{C.4})$$

The interest of this calculation then becomes clearer since the general case ( $n$ ) is treated exactly in the same way than the  $n=2$  one. More precisely, it only involves the elementary (sub)-determinants  $\det(\mathbf{M}_1, \mathbf{M}_2, \mathbf{N}_2, \mathbf{E}_4)$ ,  $\det(\mathbf{M}_1, \mathbf{E}_3, \mathbf{E}_4, \mathbf{N}_2)$  and  $\det(\mathbf{M}_1, \mathbf{E}_3, \mathbf{E}_4, \mathbf{M}_2)$  thus yielding

$$\det \left( \sum_{i=1}^n J_{\mathbf{X}} \mathbf{Y}_i(\mathbf{X}) J_{\mathbf{X}} \mathbf{Y}_i(\mathbf{X})^T \right) = P(n) \frac{d^4}{v^8} + Q(n) \frac{d^2}{v^6}. \quad (\text{C.5})$$

The case of a triangle network is treated in the same way. More precisely, we have

$$\begin{aligned} [J_{\hat{\mathbf{X}}} \mathbf{Y}_1(\mathbf{X}), J_{\hat{\mathbf{X}}} \mathbf{Y}_2(\mathbf{X}), J_{\hat{\mathbf{X}}} \mathbf{Y}_3(\mathbf{X})] &= [\mathbf{M}_1, \mathbf{E}_3, \mathbf{E}_4 : \mathbf{M}_1 + \delta_{1,2}\mathbf{M}_2, \mathbf{E}_3, \mathbf{E}_4 \\ &\quad + \delta_{1,2}\mathbf{N}_2; \mathbf{M}_1 + \delta_{1,3}\mathbf{M}_3, \mathbf{E}_3, \mathbf{E}_4 + \delta_{1,3}\mathbf{N}_3], \end{aligned}$$

where

$$\begin{aligned} (\delta_{1,2} = d_{1,2}/v^2) : \\ \mathbf{M}_2 = \begin{pmatrix} 0 \\ \sin(\theta - a_{1,2}) \\ -\cos(\theta - a_{1,2}) \\ 0 \end{pmatrix}, \quad \mathbf{N}_2 = \begin{pmatrix} 0 \\ -\cos(\theta - a_{1,2}) \\ -\sin(\theta - a_{1,2}) \\ 0 \end{pmatrix}. \end{aligned} \quad (\text{C.6})$$

For the sake of brevity, vectors  $\mathbf{M}_3$  and  $\mathbf{N}_3$  are not detailed. They are identical to  $\mathbf{M}_2$  and  $\mathbf{N}_2$ ,  $a_{1,2}$  being replaced by  $a_{1,3}$ . The rest of the calculation of  $\det(\text{FIM})$  is quite similar to the previous one, again the Binet formula [6] is the workhorse.

#### Appendix D. On the convergence of iterative methods

The aim of this appendix is to investigate the convergence of an iterative algorithm for global fusion (see Section 4.4). For this Appendix we consider that  $\mathbf{X}$  and  $\hat{\mathbf{X}}$  are *generic* (target state) vectors. Consider the functional  $J_1(\mathbf{X}) \triangleq \|\mathbf{Y}_1(\hat{\mathbf{X}} - \mathbf{Y}_1(\mathbf{X}))\|^2$ . We denote  $\hat{\mathbf{X}}$ , the exact vector of target trajectory parameters. Elementary calculations yield

$$\begin{aligned} (\mathbf{X} - \hat{\mathbf{X}})^T \nabla J_1(\mathbf{X}) &= \frac{1}{v} (\widetilde{cpa}_1 - cpa_1) (\tilde{\alpha}_1 - \alpha_1) - \frac{cpa_1}{v^2} (\tilde{v} - v) (\tilde{\alpha}_1 - \alpha_1) \\ &\quad + (\tilde{\theta}_1 - \theta_1)^2 + (\widetilde{t_{cpa}_1} - t_{cpa_1})^2 \\ &= \left( \frac{\tilde{v}}{v} \right) (\tilde{\alpha}_1 - \alpha_1)^2 + (\tilde{\theta}_1 - \theta_1)^2 + (\widetilde{t_{cpa}_1} - t_{cpa_1})^2. \end{aligned} \quad (\text{D.1})$$

The above equality is important since it proves that the following inequality holds *whatever* the  $\mathbf{X}$  vector is:

$$\forall \mathbf{X} \quad (\mathbf{X} - \hat{\mathbf{X}})^T \nabla J_1(\mathbf{X}) \geq 0. \quad (\text{D.2})$$

Note that  $(\mathbf{X} - \hat{\mathbf{X}})^T \nabla J_1(\mathbf{X})$  can be zero only if the following equalities hold  $\{\hat{\theta}_1 = \theta_1, \hat{\alpha}_1 = \alpha_1, \hat{t}_{cpa_1} = t_{cpa_1}\}$ . Similarly, define  $J_2(\mathbf{X}) \triangleq \|\hat{\mathbf{Y}}_2 - \mathbf{Y}_2(\mathbf{X})\|^2$ , then

$$\nabla J_2(\mathbf{X}) = \begin{pmatrix} \frac{1}{v} (\tilde{\alpha}_2 - \alpha_2) \\ -\frac{\alpha_2}{v} (\tilde{\alpha}_2 - \alpha_2) - \frac{d}{v^2} \cos(\theta) (\widetilde{t_{cpa_2}} - t_{cpa_2}) \\ -\frac{d}{v} \cos(\theta) (\tilde{\alpha}_2 - \alpha_2) - \frac{d}{v} \sin(\theta) (\widetilde{t_{cpa_2}} - t_{cpa_2}) \\ (\widetilde{t_{cpa_2}} - t_{cpa_2}) \end{pmatrix}. \quad (\text{D.3})$$

From Eqs. (D.2) and (D.3), we deduce that  $\nabla J_1(\mathbf{X})$  and  $\nabla J_2(\mathbf{X})$  can be *simultaneously* zeroed only if  $\mathbf{X} = \hat{\mathbf{X}}$ , which ends the proof. Thus, it has been shown that *under the valid association assumption* an iterative

algorithm has a unique stationarity point, which will be asymptotically the exact vector of parameters.

### Appendix E. On the asymptotic distribution of $F(\hat{v})$

Let  $F(\hat{v})$  be (implicitly) defined by

$$F(\hat{v}) \triangleq \Delta \hat{\mathbf{Y}}_{1,2}(\hat{v})^T \Gamma^{-1}(\hat{v}) \Delta \hat{\mathbf{Y}}_{1,2}(\hat{v}),$$

where  $\hat{v} \in \arg \min_v [F(v) + \ln(2\pi \det(\Gamma(v)))]$ . (E.1)

Now, since  $\Delta \hat{\mathbf{Y}}_{1,2}(\hat{v})$  is a maximum likelihood estimator, it converges in probability toward the zero vector. Similarly, the matrix  $\hat{\Gamma}(\hat{v})$  converges in probability toward the matrix  $\Gamma(v)$ . Thanks to Slutsky's theorems [10], we infer that  $F(\hat{v})$  is asymptotically Chi-square distributed.

### Appendix F. On the distribution of $\tan(\hat{\theta}_f)$

In (4.24), it has been shown that the track association fusion rule is based upon the following estimate of the (fused) target heading:

$$\tan(\hat{\theta}_f) = \frac{\hat{\alpha}_1 - \hat{\alpha}_2}{\hat{t}_{cpa_2} - \hat{t}_{cpa_1}}. \quad (\text{F.1})$$

Now, since the  $\{\hat{\alpha}_i\}$  and  $\{\hat{t}_{cpa_2}, \hat{t}_{cpa_1}\}$  can be reasonably assumed as normal, we are interested by the calculation of the density of the ratio of two normal random variables  $x_1$  and  $x_2$ , i.e.  $q = \frac{x_1}{x_2}$ . When both random variables  $x_1, x_2$  are centered this is a classical calculation, the density of  $q$  is a Cauchy density. If not, this is less classical and we shall present the main steps of the calculation essentially excerpted from [8]. In a first time, assume that  $x_1$  and  $x_2$  are independent, and  $x_i \sim \mathcal{N}(m_i, \sigma_i)$  ( $i = 1, 2$ ). We then denote  $a_1 \triangleq \frac{m_1}{\sigma_1}, a_2 \triangleq \frac{m_2}{\sigma_2}$ . The density  $f_v$  of the  $\mathbf{v} \triangleq (x_1, x_2)^T$  vector is thus

$$f_v(x_1, x_2) = \frac{1}{2\pi\sigma_1\sigma_2} \exp \left[ -\frac{1}{2} \left( \frac{(x_1 - m_1)}{\sigma_1} \right)^2 + \left( \frac{(x_2 - m_2)}{\sigma_2} \right)^2 \right].$$

Naturally, the following change of variable is considered<sup>11</sup>:

$$\begin{cases} x_1 = uv \\ x_2 = v \end{cases} \quad \text{whose Jacobian is: } |J| = \begin{vmatrix} v & u \\ 0 & 1 \end{vmatrix} = |v|. \quad (\text{F.2})$$

Thus, the density of the  $\mathbf{w} \triangleq (u, v)^T$  vector is simply

$$f_w(u, v) = \frac{|v|}{2\pi\sigma_1\sigma_2} \exp \left[ -\frac{1}{2} \left( \frac{(uv - m_1)}{\sigma_1} \right)^2 + \left( \frac{(v - m_2)}{\sigma_2} \right)^2 \right].$$

<sup>11</sup> Note that with this change  $u$  is the ratio  $\frac{x_1}{x_2}$ .

Marginalizing, we obtain

$$f_u(u) = \int_{\mathbb{R}} f_w(u, v) dv = \frac{1}{2\pi\sigma_1\sigma_2} \int_{\mathbb{R}} |v| \exp \left[ -\frac{1}{2} (\alpha^2(u)v^2 - 2\beta(u)v + \gamma) \right] dv$$

with  $\alpha^2(u) = \frac{u^2}{\sigma_1^2} + \frac{1}{\sigma_2^2}$ ,  $\beta(u) = \frac{m_1 u}{\sigma_1^2} + \frac{m_2}{\sigma_2^2}$ ,  $\gamma = a_1^2 + a_2^2$ , so that, finally

$$f_u(u) = \frac{e^{-\gamma/2}}{\pi\sigma_1\sigma_2\alpha^2} \int_0^\infty t e^{-t^2/2} \text{ch} \left( \frac{\beta(u)}{\alpha(u)} t \right) dt. \quad (\text{F.3})$$

Integrating by parts  $f_u(u)$ , we obtain

$$f_u(u) = \frac{e^{-\gamma/2}}{\pi\sigma_1\sigma_2\alpha^2(u)} \left( 1 + \lambda(u) e^{-\lambda(u)^2/2} \int_0^{\lambda(u)} e^{-t^2/2} dt \right)$$

with  $\lambda(u) = \frac{a_1\sigma_2 u + a_2\sigma_1}{\sqrt{(\sigma_2^2 u^2 + \sigma_1^2)}}. \quad (\text{F.4})$

### References

- [1] F.X. Bostick, H.W. Smith, J.E. Boeth, The detection of ULF, ELF emissions of moving ships. Final report, AD A 037 830, Electrical Engineering Research Laboratory, University of Texas, Austin, TX, 1977.
- [2] Y.T. Chan, G.H. Niezgod, S.P. Morton, Passive sonar detection and localization by matched velocity filtering, IEEE J. Ocean. Eng. 20 (3) (1995) 179–188.
- [3] B.V. Dasarthy, Sensor fusion potential exploitation-innovative architectures and illustrative applications, Proc. IEEE (January 1997) 24–38.
- [4] R. Donati, J.-P. Le Cadre, Detection of oceanic electric fields based on the generalized maximum likelihood ratio test, IEE Proc. Radar, Sonar Navigat. 149 (05) (2002) 221–230.
- [5] M. Duarte, Y.-H. Hu, Distance based decision fusion in a distributed wireless sensor network, Telecom Syst. 26 (2–3) (2001) 339–350.
- [6] C.H. Edwards, Advanced Calculus of Several Variables, Dover Publications, New York, 1994.
- [7] A. Farina, R. Miglioli, Association of active and passive tracks for airborne sensors, Signal Process. 69 (1998) 209–217.
- [8] M. Jay, P.L. Hennequin, Etude de la loi de probabilité de la variable aléatoire quotient de deux variables gaussiennes indépendantes, Bull. APMEP 413 (1997) 747–760.
- [9] N.L. Johnson, L. Kotz, in: Distributions in Statistics: Continuous Univariate Distributions 1–2. Wiley Series in Probability and Mathematical Statistics, Wiley, New York, 1970, Chapter 28, pp 130–145.
- [10] A.F. Karr, ProbabilitySpringer texts in statistics, Springer-verlag, Berlin, 1993.
- [11] B.O. Koopman, Search and screening, General Principles with Historical Applications, MORS Heritage Series, Alexandria, VA, 1999.
- [12] J.-P. Le Cadre, Properties of estimability criteria for target motion analysis, IEE Proc. Radar, Sonar Navigat. 145 (2) (1998) 92–99.
- [13] R. Mucci, J. Arnold, Y. Bar-Shalom, Track segment association with a distributed field of sensors, Proc. ICASSP 86 (1986).

- [14] R. Niu, P.K. Varshney, M. Moore, D. Klamer, Decision fusion in a wireless sensor network with a large number of sensors, in: *Proceedings of the Seventh International Conference on Information Fusion*, 28 June–1 July 2004, Stockholm, Sweden, pp. 21–28.
- [15] H.V. Poor, *An Introduction to Signal Detection and Estimation*, second ed., Springer-Verlag, Berlin, 1994.
- [16] B.G. Quinn, Doppler speed and range estimation using frequency and amplitude estimates, *J. Acoust. Soc. Am.* 98 (5) (November 1995) 2560–2566, Pt. 1.
- [17] B.F. La Scala, A. Farina, Choosing a track association method, *Inform. Fus.* 3 (2002) 119–133.
- [18] B. La Scala, A. Farina, Effects of cross-covariance and resolution on track association, in: *International Conference on Information Fusion*, Paris, France, 10–13 July 2000.
- [19] O. Tremois, J.-P. Le Cadre, Target motion analysis with multiple arrays: performance analysis, *IEEE Trans. Aerospace Electron. Syst.* 32 (3) (1996) 1030–1046.
- [20] D.H. Wagner, W.C. Mylander, T.J. Sanders (Eds.), *Naval Operations Analysis*, third ed., Naval Institute Press, Annapolis, MD, 1999.
- [21] G.-H. Wang, S.-Y. Mao, Y. He, Analytical performance evaluation of association of active and passive tracks for airborne sensors, *Signal Process.* 83 (2003) 973–981.
- [22] T.A. Wettergren, *Statistical analysis of detection performance for large distributed sensor systems*, NUWC-NPT Technical Report 11,436, June 2003, Newport, RI.
- [23] T.A. Wettergren, R.L. Streit, J.R. Short, Tracking with distributed sets of proximity sensors using geometric invariants, *IEEE Trans. Aerospace Electron. Syst.* 40 (4) (2004) 1366–1374.